# Phylogenomic analyses of non-Dikarya fungi supports horizontal gene transfer driving diversification of secondary metabolism in the amphibian gastrointestinal symbiont, *Basidiobolus*

Javier F. Tabima[1]

Ian A. Trautman[1]

Ying Chang[1]

Yan Wang[2,3,4]

Stephen Mondo[5]

Alan Kuo[5]

Asaf Salamov[5]

Igor V. Grigoriev[5,6]

Jason E. Stajich[2,3]

Joseph W. Spatafora[1]

**Affiliations:**

1. Department of Botany and Plant Pathology, College of Agricultural Sciences, Oregon State University, Corvallis, USA
2. Department of Microbiology and Plant Pathology, University of California—Riverside, Riverside, California, USA
3. Institute for Integrative Genome Biology, University of California—Riverside, Riverside, California, USA
4. Current address: Department of Biological Sciences, University of Toronto Scarborough, Toronto, Ontario, Canada and the Department of Ecology and Evolutionary Biology, University of Toronto, Toronto, Ontario, Canada

5. US Department of Energy Joint Genome Institute, Lawrence Berkeley National Laboratory, Berkeley, California, USA

6. Department of Plant and Microbial Biology, University of California-Berkeley, Berkeley, California, USA

**Abstract**

Research into secondary metabolism (SM) production by fungi has resulted in the discovery of diverse, biologically active compounds with significant medicinal applications. However, the fungi rich in SM production are taxonomically restricted to Dikarya, two phyla of Kingdom Fungi, Ascomycota and Basidiomycota. Here, we explore the potential for SM production in Mucoromycota and Zoopagomycota, two phyla of nonflagellated fungi that are not members of Dikarya, by predicting and identifying core genes and gene clusters involved in SM. The majority of non-Dikarya have few genes and gene clusters involved in SM production except for the amphibian gut symbionts in the genus *Basidiobolus*. *Basidiobolus* genomes exhibit an enrichment of SM genes involved in siderophore, surfactin-like, and terpene cyclase production, all these with evidence of constitutive gene expression. Gene expression and chemical assays confirm that *Basidiobolus* has significant siderophore activity. The expansion of SMs in *Basidiobolus* are partially due to horizontal gene transfer from bacteria, likely as a consequence of its ecology as an amphibian gut endosymbiont.

## Introduction

Fungi produce a wealth of biologically active small molecules – secondary or specialized metabolites – that function in interactions with other organisms, environmental sensing, growth and development, and numerous other processes (Rokas et al. 2020). Several of these compounds have led to the successful development of pharmaceuticals (e.g., antibiotics, immunosuppressants, statins, etc.) that have had dramatic and positive impacts on human health. Understanding the evolution of fungal secondary metabolites and linking them with their ecological and physiological functions in nature can inform searches for compounds with applications in human society.

Secondary metabolism (SM) is imprecisely defined but can be characterized generally as the production of bioactive compounds that are not part of primary metabolism and that are not required for growth and survival in the laboratory (Keller et al 2005, Brakhage 2013, Rokas et al. 2020). In fungi, the genes responsible for the synthesis of secondary metabolites are frequently co-located in biosynthetic gene clusters (Smith et al. 1990, Brakhage 2013), which contain the genes that control regulation of expression, biosynthesis, tailoring, and transport of these compounds out of the cell (Smith et al. 1990, Keller et al 2005, Osbourn 2010). In the kingdom Fungi, the diversity of products synthesized via SM is substantial and primarily includes alkaloids, peptides, polyketides, and terpenes (Collemare et al. 2008, Helaly et al. 2018). Each of these groups of compounds are synthesized by core genes that are characteristic of the pathways and include, but are not limited to, dimethylallyl tryptophan synthases (DMAT), non-ribosomal peptide synthetases (NRPS), polyketide synthetases (PKS), and terpene cyclases (TC). These bioactive compounds fulfill various roles that are hypothesized to increase the fitness of the fungus by promoting better recognition and adaptation to environmental cues.

Biosynthesis of secondary metabolites is heterogeneous across the fungal tree of life, but the vast majority of discovered and predicted secondary metabolites are reported within the fungal phyla Ascomycota and Basidiomycota of the subkingdom Dikarya. Filamentous ascomycetes are the major producers of secondary metabolites (e.g., penicillin, cyclosporin, etc.), with the majority of genes and gene clusters involved in fungal SM discovered in the subphylum Pezizomycotina (Collemare et al. 2008, Helaly et al. 2018). Although less than Ascomycota, Basidiomycota is also a prominent producer of SM, including some of the better-known hallucinogens (e.g., psilocybin of *Psilocybe*; Reynolds et al. 2018) and compounds toxic to humans (e.g., amanitin of *Amanita*; Luo et al. 2010).

For reasons that are unclear, the remainder of kingdom Fungi is characterized by a paucity of secondary metabolites (Voight et al. 2016). This includes the zoosporic fungi and relatives classified in Blastocladiomycota, Chytridiomycota and Rozellomycota, and the nonflagellated, zygomycete fungi of Mucoromycota and Zoopagomycota. This pattern of SM diversity supports the hypothesis that diversification of secondary metabolism is a characteristic of Ascomycota and Basidiomycota (subkingdom Dikarya), which share a more recent common ancestor relative to the other phyla. Recent genome sampling efforts have focused on increased sequencing of non-Dikarya species (Nagy et al. 2014, Kohler et al. 2015, Spatafora et al. 2016, Quandt et al. 2017, Ahrendt et al. 2018). These efforts have provided a better understanding of the relationships of the phyla of kingdom Fungi (e.g., Spatafora et al. 2016), and processes and patterns that shaped the evolution of morphologies (e.g., Nagy et al. 2014) and ecologies (e.g., Chang et al. 2019, Quandt et al. 2017) within the kingdom. The availability of a diversity of these genomes provides an opportunity to characterize and focus on the secondary metabolism composition of non-Dikarya taxa, which have remained relatively unexplored.

While the majority of non-Dikarya taxa have low SM diversity, genomic sequencing of the genus *Basidiobolus* (Phylum Zoopagomycota) revealed that it possesses an unusually large composition of SM gene clusters. Species of *Basidiobolus* have complex life cycles, which produce multiple spore types that occur in multiple environmental niches. These species are symbionts found in the digestive tracts of reptiles and amphibians, but their function and impact on the host remains unknown. The fungus is dispersed with the feces where it sporulates producing both forcibly discharged asexual spores (blastoconidia) and passively dispersed asexual spores (capilloconidia) that adhere to exoskeletons of small insects. These insects are consumed by insectivorous amphibians, completing the life cycle. *Basidiobolus* also reproduces sexually through the production of zygospores (meiospores) either by selfing (homothallic) or outcrossing (heterothallic) according to species. The fungus is also isolated from leaf litter and can be maintained in pure culture, findings that are consistent with a saprobic (decomposition of organic matter) phase to the life cycle. *Basidiobolus* must have adapted for survival in numerous environmental niches including the amphibian digestive system, amphibian feces, insect phoresis, and on decaying plant matter or leaf litter.

In this study we demonstrate that the genomes of *Basidiobolus* contain a larger number of genes related to SM than predicted by phylogeny and that in several cases the evolution of many of these SM genes is inconsistent with vertical evolution. Our objectives were to: i) characterize the diversity of SM in *Basidiobolus*, ii) identify the phylogenetic sources of this diversity, and iii) determine which classes of SM gene clusters are functional and may predict the secondary metabolites produced by species of *Basidiobolus*. Finally, we propose a model in which the amphibian gastrointestinal system is an environment that promotes noncanonical evolution of its fungal inhabitants.

## Results

*Secondary metabolite gene cluster prediction.* – A total of 38 secondary metabolism (SM) gene clusters and 44 SM core genes were predicted in the *B. meristosporus* CBS 931.73 genome, 40 SM gene clusters and 44 SM core genes for *B. meristosporus* B9252, and 23 SM gene clusters and 23 SM core genes for *B. heterosporus* B8920 (Table 1; Supplementary Table 2). Seventy-eight percent of the SM gene models predicted were found to be shared across the *Basidiobolus* isolates. Ten SM core genes were found to be unique to *B. meristosporus* CBS 931.73, 10 SM genes unique to *B. meristosporus* B9252, and 5 SM genes unique to *B. heterosporus* B8920 (Additional file 1).

A total of 721 SM gene clusters were predicted for the 66 additional Mucoromycota and Zoopagomycota genomes including 74 non-ribosomal peptide synthetases (NRPS), 167 NRPS-like, 97 polyketide synthases (PKS), 91 PKS-like, 292 terpene cyclase (TC) gene models across both phyla (Figure 1, Supplementary Table 2). For Zoopagomycota (including *Basidiobolus*), 284 SM gene models were predicted, including one NRPS-PKS hybrid, 71 NRPS, 56 NRPS-Like, 54 PKS, 46 PKS-Like, and 56 TC gene models. In Mucoromycota, 563 total SM gene models were predicted, including 45 NRPS, 142 NRPS-Like, 49 PKS, 51 PKS-Like, and 256 TC gene models. The three isolates with the most numerous predicted SM gene clusters, not including *Basidiobolus* genomes, were *Dimargaris cristalligena* RSA 468 with 33 predicted SM proteins (21 NRPS, 7 NRPS-Like, 2 PKS-Like, 3 TC), *Linderina pennispora* ATCC 12442 V 1.0 with 23 SM predicted (1 NRPS, 15 PKS, 3 PKS-like, 4 TC), and *Martensiomyces pterosporus* CBS 209.56 v1.0 with 23 SM proteins predicted (1 NRPS, 5 PKS, 14 PKS-Like, 3 TC). No DMAT gene models were predicted for any member of Mucoromycota or Zoopagomycota.

*Expression of core SM genes in* Basidiobolus. – A total of 83.45% of the RNA sequenced reads were mapped uniquely to the reference genome of *B. meristosporus* CBS 931.73, while 12.08% of the reads were mapped in more than one location. Only 4.47% of the RNA sequenced reads did not map to the reference genome. The majority of predicted SM for *B. meristosporus* CBS 931.73 were expressed at the same or higher levels than constitutive housekeeping genes, such as Beta-tubulin, Elongation Factor 1, Actin, and Ubiquitin (Figure 2). The highest expressed SM core genes per SM group were: NRPS – gene model 387529 (Cluster 5) with 74.03 transcripts per million (TPM) mapped; NRPS-like – gene model 221915 (Cluster 20) with 45.58 TPM mapped; PKS – gene model 290138 (Cluster 37) with 687.55 TPM mapped; PKS-like – gene model 207695 (Cluster 38) with 26.15 TPM mapped, and Terpene cyclase – gene model 301341 (Cluster 13) with 78.26 TPM mapped.

*Phylogenetic analysis of NRPS/NRPS-Like A-domains.* – The phylogenetic reconstruction of A-domains was performed with 951 A-domains from a combined dataset including the A-domain dataset from Bushley and Turgeon (2010) and the predictions of NRPS/NRPS-like A-domains from Mucoromycota and Zoopagomycota genome sequences (Additional file 2). A total of 395 NRPS A-domains were predicted for *Basidiobolus*, Mucoromycota and Zoopagomycota genome sequences (Additional File 3). The phylogenetic analyses recovered the nine major families reported by Bushley and Turgeon (2010) with the addition of the two new clades, surfactin-like and ChNSP 12-11-like, reported here. The total number of Mucoromycota/Zoopagomycota A-domains and their distribution across these clades are as follows: 74 to the AAR clade; 115 to the major bacterial clade (MBC), including 104 A-domains with the surfactin-like clade with and an

164 additional 11 A-domains scattered elsewhere in the MBC; the CYCLO clade with eight A-
165 domains; 65 A-domains to the ChNSP 12-11-like clade; 25 A-domains to the ChNSP 12-11
166 clade; 11 A-domains to the PKS/NRPS clade; 16 A-domains to the SID clade; 76 A-domains to
167 the SIDE clade; and 5 A-domains to the EAS clade (Figure 3). No A-domains were clustered
168 into the ACV clade or the ChNSP 10 clade, and the remaining A-domains grouped within the
169 outgroup clade (Figures 3 and 4, Supplementary Figure 1). Similar phylogenetic origins for
170 multiple A-domains were found in a single NRPS core gene (Figure 4).
171 Of fungi classified in Mucoromycota or Zoopagomycota, *Basidiobolus* genomes
172 contained the most A-domains clustered in the EAS, SIDE, and CYCLO clades. The A-domains
173 clustered within EAS represent two domains from *B. meristosporus* CBS 931.73, and one A-
174 domain of *Rhizophagus irregularis* DAOM 197198 v2.0. The A-domains clustered within SIDE
175 represent 76 domains, 44 from *B. meristosporus* CBS 931.73, 19 from *B. meristosporus* B9252,
176 and 13 from *B. heterosporus.* The A-domains clustered within the CYCLO clade represent six
177 domains, four from *B. meristosporus* CBS 931.73 and two from *B. meristosporus* B9252. The
178 NRPS A-domains grouped in the CYCLO cluster correspond to cluster 5 NRPS from *B.*
179 *meristosporus* CBS 931.73 (Protein ID 387529) and cluster 9 of *B. meristosporus* B9252
180 (Protein ID N161_4477). Gene model 387529 was predicted as a tetra-modular protein, with two
181 N-methyltransferase domains and a thioesterase domain. In addition, AntiSMASH analyses
182 predict a six gene cluster (cluster 5) that includes gene model 387529, a zinc finger transcription
183 factor (312194), carrier protein (277549), transporter (277552), peptidase (277554), and a
184 SNARE associated protein (334759) (Supplementary Figure 2). All of these gene models have
185 evidence of gene expression (Figure 2).

186 The *Basidiobolus* NRPS A-domains clustered in the surfactin-like clade included 32 A-
187 domains from eight gene models from *B. meristosporus* CBS 931.73. These included gene
188 model 375475 (Cluster 19) with eight A-domains, gene models 307892 (Cluster 33) and 343011
189 (Cluster 35) with seven A-domains each; gene model 368581 (Cluster 8) with three A-domains;
190 gene models 337511 (Cluster 16), 372991 (Cluster 17), and 298977 (Cluster 7) each with two A-
191 domains; and gene model 322666 (Cluster 2) with one A-domain. *B. meristosporus* B9252
192 contained two surfactin-like A-domains from one gene model (N161_8304; Cluster 18). *B.*
193 *heterosporus* possessed 13 A-domains from seven gene models, including N168_07733 (Cluster
194 6), N168_06479 (Cluster 13), N168_02885 (Cluster 1) and N168_00034 (Cluster 14) with two
195 A-domains each, and gene models N168_05934 (Cluster 8), N168_04239 (Cluster 12) and
196 N168_07140 (Cluster 9) with one A-domain each.
197
198 *Evolutionary relationships of predicted PKSs.* – A total of 421 KS domains were included in the
199 phylogenetic reconstruction (Additional File 4). Two KS domains were predicted from
200 Chytridiomycota genomes, 21 from Neocallimastigomycota, 46 from Basidiomycota, 78 from
201 Ascomycota, 54 from Mucoromycota, and 76 from Zoopagomycota for a total of 310 predicted
202 fungal KS domains from genome sequences (Additional File 4). The additional KS domains
203 were obtained from Kroken et al. (2003). For Mucoromycota and Zygomycota, the genomes with
204 the highest number of KS domains were *Linderina pennispora* ATCC 12442 v1.0 (20 KS
205 domains), *Coemansia spiralis* RSA 1278 v1.0 (11 KS domains), *Martensiomyces pterosporus*
206 CBS 209.56 v1.0 (10 KS domains), *Coemansia reversa* NRRL 1564 v1.0 (8 KS domains),
207 *Coemansia mojavensis* RSA 71 v1.0 (7 KS domains), and the *Basidiobolus* genomes: *B.*

208 *meristosporus* CBS 931.73 (5 KS domains), *B. meristosporus* B9252 (4 KS domains), and *B.*
209 *heterosporus* (3 KS domains).

210 Five major clades of PKS proteins were reported by Kroken et al. (2013) and recovered
211 by this study, including the fungal reducing (R) PKS, animal fatty acid synthases (FAS), fungal
212 non-reducing (NR) PKS, bacterial PKS, and fungal FAS (Supplementary Figures 3 and 4). The
213 Fungal reducing PKS1 clade included domains from *B. meristosporus* CBS 931.73 (2 KS
214 domains) and *B. meristosporus* B9252 (2 KS domains), as well as a new sub-clade called
215 "reducing PKS clade V". This clade comprised KS domains from Basidiomycota,
216 Neocallimastigomycota and one Chytridiomycota representative. No KS domains of
217 Mucoromycota or Zoopagomycota genomes were clustered within the animal FAS clade. The
218 Fungal NR PKS clade contained a new clade, "non-reducing PKS proteins clade IV", comprising
219 KS domains from Basidiomycota, Neocallimastigomycota, and one KS domain of *B.*
220 *meristosporus* B9252. The Bacterial PKS clustered KS domains from *B. meristosporus* CBS
221 931.73 (1 KS domain) and *B. meristosporus* B9252 (1 KS domain) as sole representative of
222 Mucoromycota and Zoopagomycota. Finally, the fungal FAS clade comprised all the remaining
223 KS domains of Mucoromycota and Zoopagomycota genomes (Supplementary Figures 3 and 4).

224 To better understand the predicted PKSs of Mucoromycota and Zoopagomycota that
225 clustered in the fungal FAS clade, the patterns of domains that comprise fungal PKS protein
226 sequences were analyzed. Predicted PKS of Ascomycota contained AT, KS and PP domains in
227 all sequences (Supplementary Figure 5). Predicted PKS from Basidiomycota contained AT and
228 KS domains in all sequences, while KR and PP domains were present on 36% of the sequences.
229 All PKS that contain a KS domain in the FAS clade are missing the PP domain. For
230 Chytridiomycota, the predicted PKS with the KS domain clustered in the Fungal (R) clade

231 contained AT, KS and DH domains, but no PP domain. Chytridiomycota PKS with KS domains
232 associated to FAS clade only possessed AT and KS domains. For Neocallimastigomycota, 100%
233 of PKS clustered in fungal R and NR clades contained AT and KS domains, however, only 5
234 PKS contained the PP domain. All Neocallimastigomycota PKS that clustered within the FAS
235 clade contained only AT and KS domains. For Mucoromycota and Zoopagomycota, 100% of
236 PKS contained either AT and/or KS domain, but no other domains (Supplementary Figure 6).
237
238 *Evolutionary relationships of predicted terpene cyclase gene models.* – A total of 1,108 terpene
239 cyclase or terpene cyclase-like gene models were identified and used for phylogenetic analyses
240 (Additional file 5). These include 256 identified in the Mucoromycota species genomes, 56 in the
241 Zoopagomycota genomes, and 401 ortholog proteins from 58 fungal genomes of Basidiomycota
242 and Ascomycota. An additional 395 TC candidates were identified in bacterial genomes from
243 RefSeq via BLASTP. The phylogenetic reconstruction of TC resulted in two main clades: an
244 outgroup clade that comprised predicted TC annotated as tRNA threonylcarbamoyladenosine
245 dehydratase and phytoene synthases, and a main ingroup TC core clade (Figure 5,
246 Supplementary Figure 7). The tRNA threonylcarbamoyladenosine dehydratase subclade
247 contained mostly bacterial sequences plus one TC gene model of *B. meristosporus* B9252 and *B.*
248 *meristosporus* CBS 931.73 each. The phytoene synthases clade comprised two subclades, one
249 clade that grouped most bacterial gene models, and a second clade clustering bacterial and
250 Mucoromycota predicted TC gene models, but no *Basidiobolus* TC core gene models were found
251 in this clade.
252 The TC core clade (Figure 5 and Supplementary Figure 7) comprised a bacterial
253 exclusive clade (Bacteria I), followed by four highly supported sub-clades containing TC core

254 genes from Mucoromycota, Zoopagomycota, and Dikarya, and are referred to here as Fungi TC
255 clades I – IV. The majority of TC genes from Mucoromycota and Zoopagomycota clustered
256 within clade Fungi TC II, which included no other fungal or bacterial TC. These genes were
257 annotated as Squalene synthetases by the *Mycocosm* genome portal.

258 The Fungi TC clades I, III and IV included mostly Mucoromycota TCs. The Fungi TC I
259 clade contained TC genes from Mucoromycota isolates, as well as TC genes from the
260 ascomycete isolates *Fusarium verticillioides* 7600 and *Hypoxylon sp*. EC38 v1.0, and the
261 basidiomycete *Suillus luteus* UH-Slu-Lm8-n1 v2.0. These gene models were annotated as
262 associated with the Ubiquitin C-terminal hydrolase UCHL1 according to the *MycoCosm* portal.
263 Fungi TC III clade also comprised mostly Mucoromycota isolates, with additional TCs from
264 Zoopagomycota isolates *Piptocephalis cylindrospora* RSA 2659 single−cell v3.0 and
265 *Syncephalis pseudoplumigaleata* Benny S71−1 single−cell v1.0. Annotations of genes in Fungi
266 TC III clade in *Mycocosm* indicated that these proteins are part of the isoprenoid/propenyl
267 synthetases, responsible for synthesis of isoprenoids. Isoprenoids play a role on synthesis of
268 various compounds such as cholesterol, ergosterol, dolichol, ubiquinone or coenzyme Q (Finn et
269 al. 2009). Finally, Fungi TC IV clade followed a similar Mucoromycota-enriched pattern with
270 the exceptions of *Dimargaris cristalligena* RSA 468 single−cell v1.0, *Linderina pennispora*
271 ATCC 12442 v1.0, *M. pterosporus* CBS 209.56 v1.0, and *Syncephalis fuscata* S228 v1.0. Fungi
272 TC IV clade also included TC genes from Ascomycete sequenced genomes. The majority of
273 these genes were annotated as containing a terpene synthase family, metal binding domain, and a
274 polyprenyl synthetase domain in the *MycoCosm* genome portal.

275 Within the fungal clades, the NADH dehydrogrenase (ubiquinone) complex clade
276 represented a highly supported clade clustering bacterial, Mucoromycota and Zoopagomycota

277 TCs. Annotations associated with gene models found in this clade indicated that this clade
278 comprised TC associated to NADH dehydrogrenase (ubiquinone) complex.
279 The terminal clades of TC clusters include the Bacteria II + *Basidiobolus* clade that
280 included bacterial TC and six TC SM core genes predicted from *Basidiobolus* (two from each
281 genome), and the clade comprising TC core genes solely from Dikarya and one gene from
282 *Mortierella verticillata NRRL 6337* and *Rhizopus microsporus ATCC11559 v1.0* (Figures 5 and
283 Supplementary Figure 7).
284
285 *Signatures for HGT in* Basidiobolus *genomes*. – The identity search for genes with evidence for
286 HGT identified 934 genes in *B. meristosporus* CBS 931.73, 620 genes of *B. meristosporus*
287 B9252, and 382 genes of and *B. heterosporus* B8920 with zero BLASTP hits to fungal proteins.
288 These genes were used for the coverage assay to identify gene model coverage deviation from
289 the harboring scaffold median coverage (Sup. Fig. 7). This assay resulted in 810 genes of *B.*
290 *meristosporus* CBS 931.73, 503 genes of *B. meristosporus* B9252, and 301 genes of and *B.*
291 *heterosporus* B8920 with z-scores under 2 standard deviations from the harboring scaffold
292 median coverage. These genes were considered candidate genes with evidence for HGT, and
293 represented 5%, 4% and 3% of the gene content of *B. meristosporus* CBS 931.73, *B.*
294 *meristosporus* B9252, and *B. heterosporus* B8920, respectively. The HGT candidates showed
295 significant differences in GC content when contrasted to genes considered of fungal origin
296 (Mean fungal GC content (expected) = 0.492, Mean HGT GC content (Observed) = 0.486, t =
297 3.4119, df = 891.77, p-value = 0.0006741), but no differences in codon usage or 5-mer
298 composition were detected between HGT candidate and fungal genes (Supplementary Figures 10
299 and 11). Differences were also found for intron number and normalized intron length between

genes HGT candidate genes and fungal genes, where the distribution of intron number shows a median of 0 introns for HGT candidates and 2 for fungal genes (Kruskal-Wallis test; $\chi^2$=272.88, df = 1, p-value < 2.2e-16; Sup. Fig. 9). The majority of HGT candidate genes (61% of the genes) have no introns, compared to 36% of genes from fungal origin with no introns (Sup. Fig. 9). The candidate HGT genes have a significantly smaller normalized intron length than the genes with a fungal origin (Kruskal-wallis test; $\chi^2$=272.88, df = 1, p-value < 2.2e-16).

A large percentage of SM core genes appeared to be the product of HGT from bacterial species into *Basidiobolus*. The SM core genes identified as candidate HGT genes is 61%, 44% and 52% for *B. meristosporus* CBS 931.73, *B. meristosporus* B9252, and *B. heterosporus* B8920, respectively (Table 2). NRPS/NRPS-like SM core genes represent the largest percentage of HGT evidence, while TC have the lowest percentage of HGT evidence (Table 2, Table 3). The identification of taxonomic sources for HGT into *Basidiobolus* indicated that most HGT comes from bacteria in the phylum Proteobacteria with 234, 160 and 95 gene models in *B. meristosporus* CBS 931.73, *B. meristosporus* B9252, and *B. heterosporus* B8920, respectively. Firmicutes (112, 63, and 39 gene models, respectively) and Actinobacteria (127, 67, and 40 gene models, respectively) (Figure 6, Supplementary Table 4) were the second and third most abundant source of HGT from bacteria into *Basidiobolus*.

Most HGT candidates genes resulted in no gene ontology (GO) annotation (659 gene models) or no InterPro domain annotation (140 gene models, Supplementary Table 5). The ten top GO terms were oxidation-reduction process (59 gene models), protein binding (34 gene models), phosphorelay sensor kinase activity (32 gene models), N-acetyltransferase activity (28 gene models), catalytic activity (26 gene models), extracellular space (25 gene models), hydrolase activity (24 gene models), oxidoreductase activity (23 gene models), hydrolase activity

(24 gene models), hydrolyzing O-glycosyl compounds(23 gene models) , and NRPS (18 gene models) (Figure 6, Supplementary Table 5).

*Siderophore activity in* Basidiobolus meristosporus. – The siderophore activity assay resulted in visible activity for the three replicates for *B. meristosporus* and *Cladosporium sp.*, and a small halo for one of the replicates of *C. thromboides*. No visible siderophore activity was detected for the other two replicates of *C. thromboides* or for the empty AY-CAS plates (Figure 7, Supplementary Figure 12). The analysis of variance for the area of siderophore activity measured showed significant differences across isolates/empty plates (ANOVA, F value = 19.62, $p$ = 0.0004). Post-hoc tests showed no differences between *B. meristosporus* and *Cladosporium sp.* siderophore activity (Tukey HSD, $p$ = 0.9801489) nor between *C. thromboides* and the empty AY-CAS plates (Tukey HSD, $p$ = 0.9396603), but significant differences were found for all other comparisons (Tukey HSD, $p < 0.001$ for all remaining comparisons).

## Discussion

Secondary, or specialized, metabolite (SM) production is an important element of fungal metabolism. It has resulted in numerous natural products with human health implications, such as mycotoxins in our food supply, and medical applications, including antibiotics, immunosuppressants, and antitumor agents. The majority of the known genetic and chemical diversity of fungal SM has been described from the phyla Ascomycota and Basidiomycota with few SM gene clusters, and limited SM production, reported for fungi in Mucoromycota and Zoopagomycota. This observation has led to the dogma that ‘zygomycete’ species are

depauperate of these chemical pathways (Voight et al. 2016). Here we report gene clusters involved in SM production in the largest survey to date of Mucoromycota and Zoopagomycota species using genomics approaches and estimate the SM potential of these fungi.

Genome sequencing of a total of 69 isolates across diverse lineages of Mucoromycota and Zoopagomycota enabled detailed identification of SM clusters. These results support the hypothesis that zygomycete fungi have a low abundance of secondary metabolism (Figure 1, Supplementary Table 2) and agree with previous reports (Voight et al. 2016). Outliers to this pattern exist, however, and are particularly true of the genus *Basidiobolus* (Zoopagomycota), which possesses a large number of SM gene clusters predicted for the NRPS, PKS and TC families. This discovery of abundant candidate genes for production of secondary metabolite in *Basidiobolus* is novel and its presence is most consistent with a signal of horizontal gene transfer from bacteria to fungi, a phenomenon we propose is facilitated by living in the amphibian gut environment.

*Distribution and Evolution of NRPS Genes Across Mucoromycota and Zoopagomycota.* – A deeper examination of *Basidiobolus* SM gene clusters indicates that this genus surpasses the number of expected NRPS genes for zygomycete species (Figure 1). Most of these SM genes also show evidence for transcription, indicating that the majority of these genes are expressed constitutively under laboratory conditions (Figure 2). Several of these core genes, such as the NRPS gene model 387529, appear to be expressed at a higher rate than several housekeeping genes.

A more detailed census of core genes reveals unique patterns of evolution of NRPS genes across Mucoromycota and Zoopagomycota when compared to Dikarya fungi (Figure 3, Table 1).

The only NRPS A-domains found throughout the two phyla are members of the AAR clade (with the exception of *Rhizopus delemar* 99-80). These A-domains are from the genes that encode α-aminoadipate reductases (AAR), an enzyme responsible for the reduction of alpha-aminoadipic acid, which is essential for the lysine biosynthesis pathway and is present in all fungal phyla (Bushley and Turgeon 2010). In contrast, the remaining NRPS genes, and their respective A-domains, show discontinuous and patchy distributions across Mucoromycota and Zoopagomycota (Figure 3).

The most pronounced NRPS diversification in *Basidiobolus* are for genes that are predicted to encode for siderophores, iron chelating metabolites. A-domains for predicted siderophores are distributed throughout four clades including the three clades of major bacterial genes and the fungal SID and SIDE clades (Figure 3, Sup. Fig. 1). Major bacterial clades (MBC) exclusively comprise bacterial siderophore synthases, such as pyoverdine, yersiniabactin and pyochelin (Bushley and Turgeon 2010), with the exception of the surfactin-like clade. Our results show that genomes of *Mortierella* and *Basidiobolus* contain A-domains that are members of the MBC, and that they are the only fungal representatives of these clades. SID clade contains all NRPS associated with siderophore production from Ascomycota and Basidiomycota species. All *Basidiobolus* isolates contain one NRPS A-domain in this clade, as well as three A-domains from three NRPS gene models of *Conidiobolus coronatus* NRRL28638. Finally, SIDE, a clade comprising NRPS genes responsible for the production of siderophores in filamentous ascomycetes is expanded in *Basidiobolus* (Figure 3), which is also the only zygomycete with A-domains clustered in this clade. These findings are consistent with enrichment of both bacterial and fungal siderophores and are suggestive of the importance of iron metabolism in *Basidiobolus*.

The CYCLO clade contains the A-domains for core genes associated with biosynthesis of cyclic peptides, such as beauvericin and cyclosporin (Bushley and Turgeon 2010, Bushley et al 2013). Sister to all other CYCLO clade A-domains are the A-domains that comprise the NRPS core gene model 387529 from *B. meristosporus* (Supplementary Figure 2). 387529 is expressed at the highest rate of any SM gene under laboratory conditions (Figure 2). It is annotated as a tetra-modular gene model, that includes two N-methylation domains, four adenylation domains, four condensation domains, and a TE domain. When compared to *simA*, the NRPS responsible for biosynthesis of cyclosporin, structural similarities can be found, such as the presence of the N-methylation domains and the TE terminator domain. Its phylogenetic and structural similarities to *simA* suggest that 387529 results in the synthesis of a cyclic peptide with methylated amino acid residues.

The surfactin-like clade contains A-domains for bacterial core genes with similarities, but not identical, to the *Bacillus subtilis* surfactin termination module (*srfA-C* gene; Peypoux et al. 1999) including the third, fourth and fifth A-domains of the five A-domain gene model NP_930489.1 of *Photorhabdus luminescens* gene, two domains of the gene PvdD (AAX16295.1; pyoverdine synthetase) of *Pseudomonas aeruginosa*, and a single A-domain of the bimodular NRPS dbhF protein of *Bacillus subtilis* (AAD56240.1) which is involved in the biosynthesis of the siderophore bacillibactin. This surfactin-like clade contains eleven A-domains predicted from *Basidiobolus* genomes including the gene models 298977, 368581 and 372991 from *B. meristosporus* CBS 931.73. Gene model 298977 showed no evidence for gene expression, while gene models 368581 and 372991 show high rates of expression (Fig. 2). This is the first report of the prediction of a surfactin-like gene in fungi, but surfactant production was recently reported in *Mortierella alpina* (Baldeweg et al. 2019). These include malpinins, amphiphilic acetylated

hexapeptides that function as natural emulsifiers during lipid secretion, and malpibaldins, hydrophobic cyclopentapeptides. This finding is consistent with the genomic data and reveals that *Mortierella*, in addition to *Basidiobolus*, possesses homologs in the surfactin-like clade that are phylogenetically different from *B. subtilis* surfactins.

Surfactins, encoded by the *srfA* gene cluster in *Bacillus subtilis*, are functionally active as surfactants, as well as toxins and antibiotics. However, the surfactin genes from *B. subtilis* (SrfA-AA, SrfA-AB and SrfA-AC) were included in our analysis and clustered in a different clade within the MBC. A-domains from single module NRPS-like protein from *B. meristosporus* CBS 931.73 (Gene model 146993) and from a NRPS-PKS hybrid A domain from of *B. meristosporus* B9252 (Gene model N161_14278) clustered with the *B. subtilis* SrfA genes. The placement of this NRPS-PKS A-domain is interesting because surfactins are lipopeptides, which contain a hydrophobic fatty acid chain, whose biosynthesis is consistent with an NRPS-PKS hybrid. The A-domains from the remaining Mucoromycota and Zoopagomycota NRPS-PKS hybrids clustered as sister to the original clade of Dikarya NRPS-PKS hybrids, supporting the hypothesis of a single origin of fungal NRPS-PKS hybrids (Bushley and Turgeon 2010).

*Mucoromycota and Zoopagomycota lack PKS diversity*. – Polyketide synthases (PKS) are abundant SM of Ascomycota and Basidiomycota and are involved in antibiotic production, carotenoid biosynthesis and other functional roles. In contrast, literature on PKS diversity for Mucoromycota and Zoopagomycota is limited. Our analyses update the phylogenetic reconstruction reported by Kroken et al. (2013) by adding genomic information from Chytridiomycota, Mucoromycota and Zoopagomycota (Supplementary Figures 3 and 4). Overall, we report the discovery of two new clades: A clade of non-reducing PKS proteins (clade IV)

438 comprising Neocastimastigomycota and Basidiomycota, and a reducing PKS clade (reducing
439 PKS clade V) consisting of Neocastimastigomycota, Chytridiomycota and Basidiomycota. The
440 results of our PKS prediction revealed a number of potential PKS core genes in zygomycete
441 species (Supplementary Figures 3 and 4), but the results of our phylogenetic reconstruction show
442 that the KS domain of the predicted PKS gene models are fungal fatty acid synthases (FAS).
443 Only *Basidiobolus meristosporus* genomes possessed KS domains associated with fungal PKS,
444 either reducing or non-reducing.

445 A domain-by-domain presence/absence analysis of PKS genes models (Supplementary
446 Figures 5 and Figure 6) shows that in addition to AT and KT domains, a third domain (either
447 KR, DH or PP) is found in the majority of fungal PKSs (Supplementary Figure 5). Conversely,
448 the zygomycete genes in the FAS clade only possess the AT and/or KT domains, which are
449 domains common between FAS and PKS, including the majority of PKSs predicted for
450 *Basidiobolus.* However, *Basidiobolus* KS domains are found in both fungal and bacterial PKS
451 clades. Gene models 292783 and 237744 from both isolates of *B. meristosporous* cluster with
452 fungal reducing PKS II and possess the DH domain (Supplementary Figure 4), and the
453 expression levels of 292783 is consistent with an actively transcribed gene (Figure 2).
454
455 *Terpene cyclase-like genes are expanded in zygomycetes.* – Terpene cyclases (TC) are the most
456 common SM predicted for zygomycete species (Figure 1, Supplementary Table 2). Phylogenetic
457 reconstruction shows that zygomycete TC core genes are clearly distinct from Ascomycota and
458 Basidiomycota TC, where at least 4 new clades of predominantly zygomycete TC are found
459 (Figure 5, Supplementary Figure 7). Fungi II TC clade comprises TC from all zygomycete
460 genomes analyzed with the exception of *Piptocephalis cylindrospora* RSA 2659 single−cell

v3.0, *Phycomyces blakesleeanus NRRL1555* v2.0, and five genomes of *Rhizophagus irregularis*, which show no prediction of TC in their genomes. No Dikarya TC genes cluster within this clade. Fungi I, III and IV group TC genes are found almost exclusively in Mucoromycota species, as well as some Dikarya species. TC genes from Fungi I are present only in Mucoromycotina genomes. Functional annotations of TC genes from this clade indicate that these TC genes code for proteins associated with squalene and phytoene synthases and are part of the synthesis of carotenoids. Carotenoids are important compounds for the synthesis pathway of trisporic acid, the main molecule responsible for initiating sexual reproduction in zygomycetes (Burmester et al. 2007). Finally, *Basidiobolus* is the only non-Dikarya genus with TC genes clustered within the Bacteria II clade of TC. Both these SM core genes show evidence for expression comparable to housekeeping genes or other SM core genes (Figure 2). The presence of bacterial-like TC genes in *Basidiobolus* present more evidence on the plasticity of the genome of *Basidiobolus* and its ability to integrate and possibly express foreign SM associated DNA.

*Horizontal Gene Transfer of SM genes to Basidiobolus? – Basidiobolus* is a genus with a complex biology, alternating ecologies, and multiple spore types. This complex biology is also reflected at the genomic scale. The sequenced genomes show a larger genome size than other zygomycetes, as well as a higher number of genes than any other Zoopagomycota genomes sequenced to date. Our SM prediction assay is concordant with these patterns in which *Basidiobolus* has an excess of SM gene clusters when compared to other zygomycetes. Evidence points to HGT as a main driver of SM diversity in *Basidiobolus* as supported by the phylogenetic reconstructions of NRPS, PKS and TC gene clusters with bacterial homologs. *Basidiobolus* and *Mortierella* are the only fungi with genes associated with the bacterial clades in each of these SM

phylogenetic reconstructions. Moreover, these HGT candidates are integrated into the *Basidiobolus* genome assembly and do not show evidence of artifactual assembly as evidenced by discontinuous coverage (Supplementary Figure 8). The most abundant functional group of SM core genes overall are siderophores and their overall functionality is supported by both the RNA expression analyses (Figure 2) and siderophore plate assays (Figure 7).

One stage of the *Basidiobolus* life cycle the fungus lives as a gut endosymbiont where it co-occurs with bacteria and other organisms that comprise the gut microbiome. Animal gut environments can facilitate HGT between bacteria and fungi, as previously reported for the zoosporic species of Neocallimastigomycetes (Chytridiomycota), which live in the ruminant gut environment and whose genomes exhibit a 2-3.5% frequency of genes with HGT evidence (Wang et al. 2018; Murphy et al. 2019). Phylogenomic analyses of the *Basidiobolus* NRPS A-domains support a phylogenetic affinity with A-domains from bacterial taxa and more rarely other fungi, a pattern most consistent with HGT. Our HGT survey comprised an extensive search of reference genomes across the tree of life available in NCBI RefSeq, as well as all of the gene models predicted for the Mucoromyocta and Zoopagomycota genomes. We find that 3% to 5% of all predicted gene models present in *Basidiobolous* genomes are consistent with signatures of HGT from bacteria. However, the percentages radically change to 41% to 66% of predicted SM core gene models with bacterial HGT evidence. These SM gene models with bacterial signatures are highly abundant, with NRPS and NRPS-like genes comprising the top 25 ontology categories of HGT genes in *B. meristosporus* (Supplementary Table 5). These results are consistent with the life history of *Basidiobolus*, where the fungus lives in close proximity with other microorganisms associated with the amphibian gut environment.

506 The additional analyses to discover distinct genetic features for HGT candidates showed
507 that the largest differences found are in intron number and intron length, but not in nucleotide
508 composition or by codon usage. A significantly smaller number of introns and smaller
509 normalized intron length in HGT candidates provide more support to the HGT hypothesis, where
510 we expected that bacterially transferred genes would maintain a smaller number and length of
511 introns. Intronic expansion of transferred genes into fungal species after an HGT event appears
512 to be rapid in order to reflect the genetic makeup across the genome (Da Lage et al. 2013) and
513 can explain the introns in some of the HGT candidates. However, up to 60% of the HGT
514 candidates still maintain absence of introns as expected for genes of bacterial origin. Finally, the
515 nucleotide composition of HGT candidates and fungal genes were indistinguishable. Reports
516 show that foreign genes with similar codon usage are more likely to become fixed on the
517 receiving genome (Medrano-Soto et al. 2004, Amorós-Montoya et al. 2010, Tuller 2011). We
518 interpet these results to indicate that horizontally transfered genes are evolving towards a similar
519 nucleotide composition of the fungal genome based on the 5-mer/codon usage assay, but still
520 maintain high protein similarity to and group with donor lineage copy in phylogenetic
521 reconstructions.

522 The taxonomic survey of our HGT analysis shows that a diverse array of bacteria may
523 have consistently contributed genetic information into the *Basidiobolus* genomes (Figure 6 and
524 Supplementary Table 4). The most abundant bacterial taxonomic groups associated with HGT
525 are the Proteobacteria, Firmicutes, Actinobacteria/high GC gram positive bacteria, and
526 Bacteriodetes (Figure 6, Supplementary Table 4). The proportion of HGT for each taxonomic
527 group appears to be consistent among the three *Basidiobolus* genomes, and there are
528 consistencies between the most common taxonomic groups responsible for HGT in *Basidiobolus*

and the reported composition of bacteria associated with the gut microbiome in amphibians (Bletz et al. 2016, Kohl et al. 2013) and reptiles (Colston and Jackson, 2016, Costello et al. 2010).

## Conclusions

Our results confirm that the majority of zygomycete fungi classified in Mucoromycota and Zoopagomycota do not possess a large genomic potential for secondary metabolism. Significant departures from this pattern exist, however, as exemplified by *Basidiobolus*, a genus with a complex genomic evolution and potential for considerable and diverse secondary metabolite production. First, it possesses larger than average genome with less than 8% content of repetitive regions, but a genetic plasticity to integrate and express extrinsic DNA. Second, the incorporation of extrinsic DNA is consistent with selection for increased SM production, especially gene models that are related to the capture of resources available in anaerobic conditions (iron chelation by siderophores) and metabolites that may play roles in antibiosis (surfactin-like genes) or host interaction. Third, the amphibian gut environment predisposes *Basidiobolus* to the acquisition of these SM core genes via HGT from co-inhabiting bacterial species. More information is needed to further test these hypotheses, including sequencing of additional *Basidiobolus* species with long read technologies; more accurate characterization of amphibian microbiomes that test positive for *Basidiobolus*; and LC-MSMS characterization of the *Basidiobolus* metabolome.

## Materials and Methods

*Data collection.* – Annotated genome and amino-acid translation of predicted gene model sequences for three isolates of two species within the genus *Basidiobolus* were used in this study*: Basidiobolus meristosporus* CBS 931.73 (Mondo et al. 2017), isolated from gecko dung in the locality of Lamco, Ivory Coast; *B. meristosporus* B9252 (Chibucos et al. 2016) isolated from human eye in Saudi Arabia; and *B. heterosporus* B8920 (Chibucos et al. 2016) isolated from plant debris in India. The genomic sequence of *B. meristosporus* CBS 931.73 was sequenced with PacBio and annotated by Mondo et al. (2017) and obtained from the US Department of Energy Joint Genome Institute *MycoCosm* genome portal (https://mycocosm.jgi.doe.gov; Grigoriev et al. 2014). Genomic sequences and annotation of *B. meristosporus* B9252 and *B. heterosporus* B8920 sequenced by Chibucos et al. (2016) were obtained directly from the authors. The raw reads for these two species are available in GenBank (Accession numbers GCA_000697375.1 and GCA_000697455.1). Data sources for the remaining genomes included in these analyses are available in Supplementary Table 1.

*Secondary metabolite gene cluster prediction.* – Secondary Metabolite gene clusters for *Basidiobolus* species were predicted with AntiSMASH v4.2.0 (Weber et al. 2017) and the Secondary Metabolite Unique Regions Finder (SMURF; Khaldi et al. 2010) from the annotated genomes of the three isolates used in this study. The AntiSMASH prediction was performed on local HPC, while SMURF predictions were obtained by submission of the genomes the SMURF web server (http://smurf.jcvi.org/). Predictions were contrasted manually to determine shared clusters of secondary metabolites. Predicted SM proteins were retrieved for the genomes of 66 additional Mucoromycota and Zoopagomycota species based on the SMURF predictions

574 available at *MycoCosm* and by local prediction with AntiSMASH. Orthologous sets of core SM
575 genes across *Basidiobolus* were identified using OrthoFinder (Emms et al. 2015).
576
577 *Secondary metabolite expression analysis.* – To assess the expression of predicted SM proteins
578 in *B. meristosporus,* we calculated summarized counts of RNA transcript per million (TPM) for
579 genes in *B. meristosporus* CBS 931.73 isolate by aligning RNA-Seq reads to the assembled *B.*
580 *meristosporus* CBS 931.73 genome with HiSat v2.1.0 (Kim et al. 2019). The aligned sequence
581 reads were processed with HTS-seq (Anders et al. 2014) to generate the counts of overlapping
582 reads found for each gene and the normalized TPM for the genes was calculated using the cpm
583 function in edgeR (Robinson et al. 2010). A distribution of RNA-Seq read counts per gene was
584 plotted using the ggplot2 package in the R statistical framework (R Core Team 2018).
585
586 *Phylogenomic analyses.* – Phylogenetic analyses were used to assess the evolutionary
587 relationships of the NRPS, PKS, and terpene cyclase/synthase predicted proteins. For the NRPS
588 genes, the adenylation domains (A-domains) were identified by hmmsearch from HMMer 3.0
589 suite (Eddy 2004), using the A-domain profile reported by Bushley and Turgeon (2010) as a
590 reference profile HMM. The predicted A domains were extracted from the resulting HMMER
591 table into a FASTA file using the esl-reformat program included in the HMMER suite. The
592 predicted A-domains for all *Basidiobolus,* Mucoromycota and Zoopagomycota species were
593 added to an A-domain amino-acid alignment reported by Bushley and Turgeon (2010) with
594 MAFFT v7 (Katoh et al. 2017) (Additional file 1). This reference alignment contains A-domains
595 from NRPS proteins from nine major subfamilies of fungal and bacterial NRPS proteins. The
596 phylogenetic domain tree was constructed using a maximum likelihood approach implemented in

RAxML v. 8.2.11 (Stamatakis et al. 2014) with the JTT amino acid substitution matrix, after model selection using the PROTGAMMAAUTO option, and 1000 bootstrap replicates (raxmlHPC-PTHREADS -T 12 -n NRPS -s infile.fasta -f a -x 12345 -p 12345 -m PROTCATJTT –N 1000). A graphical representation of the A-domains from the NRPS/NRPS-like core gene models (Fig. X) was constructed by coloring the A-domain position in the core gene according to its phylogenetic origin using the ggplot2 R package (Wickham, 2016).

For the PKS genes, the KS domains of all predicted PKS proteins from the *Basidiobolus*, Mucoromycota and Zoopagomycota species were identified using hmmsearch, using the KS domain profile (PF001009) available in PFAM v31 (Finn et al. 2009). The predicted KS domains for all *Basidiobolus*, Mucoromycota and Zoopagomycota species were added to an existing KS domain amino-acid alignment reported by Kroken et al. (2003) using MAFFT v7 (Katoh et al. 2017) (Additional file 2). This existing alignment contained KS domains from PKS proteins from reduced and unreduced PKS from bacterial and fungal species. The Kroken et al. (2003) database was expanded by adding predicted KS domains from PKS proteins of additional published fungal genomes in order to include more fungal diversity in the dataset: Eight Ascomycota isolates (*Aspergillus nidulans* FGSC A4, *Beauveria bassiana* ARSEF 2860, *Capronia coronata* CBS 617.96, *Capronia semiimmersa* CBS 27337, *Cladophialophora bantiana* CBS 173.52, *Cochliobolus victoriae* FI3 v1.0, *Microsporum canis* CBS 113480, *Trichoderma atroviride* v2.0), nine Basidiomycota isolates (*Acaromyces ingoldii* MCA 4198 v1.0, *Fibroporia radiculosa* TFFH 294, *Fomitiporia mediterranea* v1.0, *Gloeophyllum trabeum* v1.0, *Gymnopus luxurians* v1.0, *Laccaria bicolor* v2.0, *Microbotryum lychnidis−dioicae* p1A1 Lamole, *Piloderma croceum* F 1598 v1.0, *Pisolithus tinctorius* Marx 270 v1.0), four Neocallimastigomycota isolates (*Anaeromyces robustus* v1.0, *Orpinomyces sp.*, *Piromyces finnis*

v3.0, *Piromyces sp. E2* v1.0) and one Chytridiomycota species (*Spizellomyces punctatus* DAOM BR117). The predicted PKS proteins from additional species were all obtained from the DOE-JGI *MycoCosm* genome portal by searching for all genes with "PKS" on the SM annotation from *MycoCosm*. The KS domains were identified for the subset of PKS proteins using a HMMER KS profile as mentioned above. A phylogenetic tree was reconstructed using maximum likelihood using all KS domains using similar parameters described in the NRPS step.

The terpene cyclase (TC) proteins were predicted in AntiSMASH for all 69 assembled genome sequences from *Basidiobolus*, Mucoromycota and Zoopagomycota. To include additional fungal TC proteins in the phylogenetic reconstruction, we identified TC proteins from 58 published genomes of Dikarya isolates (21 Basidiomycetes and 37 Ascomycetes) available in DOE-JGI *MycoCosm*, each from a different family (Supplementary Table 3). One isolate per family was randomly selected for the analysis. To screen for TC proteins in Dikarya, OrthoFinder was used to build orthologous clusters of genes between *Basidiobolus*, Mucoromycota and Zoopagomycota TC and the Dikarya proteome dataset. Dikarya proteins clustered within orthologous groups that contain TC of *Basidiobolus*, Mucoromycota and Zoopagomycota were considered valid TC orthologs and used in downstream analyses. Finally, we identified bacterial TC to evaluate the potential for HGT into *Basidiobolus*, Mucoromycota or Zoopagomycota species. Bacterial TC's were identified by screening each protein from the RefSeq, release 87 (May 2018, O'Leary et al. 2016) FASTA dataset against a BLAST database (Altschul et al. 1997), one from each of the zygomycete orthologous groups identified by OrthoFinder in the previous step, for a total of four protein sequences in the database. The BLASTP program was used to perform the searches, using an e-value of $1e^{-10}$ and the BLOSUM62 substitution matrix. Positive matches from the BLASTP assay were used as

643 bacterial TC for subsequent analyses. A multi-sequence alignment containing all predicted TC
644 from *Basidiobolus*, Mucoromycota and Zoopagomycota species, the orthologous TC from
645 additional fungal species, and the TC proteins from reference bacterial predicted gene models
646 result of the BLASTP search was performed in MAFFT v7 using the G-INS-1 algorithm for
647 progressive global alignment (Katoh et al. 2017) (Additional file 3). A phylogenetic tree was
648 reconstructed using maximum likelihood in RAxML using similar parameters as mentioned
649 before.
650
651 *Horizontal gene transfer in* Basidiobolus *species.* – Identification of genic regions with evidence
652 for horizontal gene transfer (HGT) from bacteria was performed by searching all translated
653 proteins from the predicted gene models of the *Basidiobolus* isolates against a custom BLAST
654 protein database. This database included all amino-acid sequences available in the NCBI RefSeq
655 proteomics database and all available amino-acid sequences for Mucoromycota and
656 Zoopagomycota species at the DOE-JGI *MycoCosm* genome portal. The proteins were searched
657 with BLASTP against the combined RefSeq/Mucoromycota/Zoopagomycota custom database,
658 using an e-value cutoff of $1e^{-10}$ and the BLOSUM62 substitution matrix. A summary of the
659 taxonomy identifier for all best hits was obtained by identifying whether the best hit was a
660 Mucoromycota/Zoopagomycota protein, or a RefSeq protein. We used the rentrez package
661 (Winter, 2017) in the R statistical framework to extract the top-ten taxonomic identifiers from
662 the NCBI database when hits did not correspond to Mucoromycota/Zoopagomycota. Proteins
663 that had no hits to a fungal protein and only hits to a bacterial protein were considered candidate
664 HGT genes.

665 To increase the accuracy of the prediction of genes product of HGT, we tested whether
666 HGT candidate genes showed signs of errant assembly or in silica incorporation into the
667 *Basidiobolus* genomes. The mean genomic read coverage of each candidate gene was calculated
668 and compared to the mean coverage of the scaffold harboring the HGT candidate gene for all
669 three *Basidiobolus* isolates. A z-score was calculated in R to determine the number of standard
670 deviations of the HGT candidate from the mean coverage of the harboring scaffold. All HGT
671 candidates with standard deviations greater or less than two were removed from the analysis.
672 The genomic reads were mapped to each reference genome using BWA (Li and Durbin, 2009).
673 Coverage per HGT and harboring scaffold was estimated using samtools (Li et al. 2009). A
674 summary plot of the proportion of genes with bacterial best hits was constructed using the
675 ggplot2 package in R.
676 To identify differences in the GC content between HGT candidates and genes of fungal
677 origin, a paired t-test was performed between the mean GC content for HGT candidates and
678 fungal genes for the predicted genes of *Basidiobolus meristosporus* CBS 931.73 as this species
679 has the genome with longest contigs and best assemblies overall. In addition, to identify if the
680 HGT candidate genes had a reduced number of introns than the fungal genes, a summary of the
681 number of introns and normalized intron length (intron length divided by gene model length) was
682 performed in the GenomicRanges R package (Lawrence et al. 2013). A Kruskal-Wallis test was
683 performed in R to identify significant differences in the number of introns and the normalized
684 intron length for the HGT candidates and the fungal genes. A nucleotide composition analysis
685 based on 5-mers and codon usage was performed to observe differences between candidate HGT
686 genes and fungal genes for *Basidiobolus meristosporus* CBS 931.73. The 5-mer analysis was
687 conducted in all predicted coding sequences from the annotated gene models using the

688 oligonucleotideFrequency function of the Biostring R package (Pagès et al. 2019). Codon usage
689 was estimated using the uco function of the seqinr R package (Charif and Lobry 2007). Both
690 these indices were divided by gene length to normalize the nucleotide composition by the effect
691 of gene length. Principal component analyses were performed in R for both 5-mer and codon
692 usage analysis to compare the HGT candidates to the fungal candidate genes. Lastly, the putative
693 functions of the genes with evidence for HGT were summarized using the functional annotations
694 available in the gene format file (GFF) of *B. meristosporus* CBS 931.73.
695
696 *Measuring siderophore activity in* Basidiobolus. – To measure the siderophore activity (chelation
697 of ferric ions) of *Basidiobolus,* an assay of detection of siderophore activity based on the
698 universal chrome azurol S (CAS) assay (Andrews et al. 2016) was performed for the strain
699 *Basidiobolus meristosporus* CBS 931.73. This colorimetric assay uses a complex of Fe(III) –
700 CAS – DDAPS (Surfactant). When this complex is combined with acetate yeast agar (AY agar),
701 it results in a greenish-blue color, where the color changes to yellow upon the removal of the
702 iron. A total of 450 ml of AY agar (Andrews et al. 2016) was mixed with 50 ml of autoclaved
703 10X CAS assay (20 ml of 10 mM $Fe(NO_3)_3$, 40 ml of 10 mM chrome azurol S, and 100 ml of 10
704 mM DDAPS). A 10 cm layer of the AY-CAS media was poured in small petri dishes and cooled.
705 An upper layer of 10 cm of AY agar was poured after cooling, and the media was left to diffuse
706 overnight and stored at 4°C for 24 hours. *B. meristosporus*, *Conidiobolus thromboides* FSU 785
707 (negative control), and *Cladosporium sp.* from the *herbarum* species complex PE-07 (positive
708 control) were transferred into the AY-CAS plates by transferring a small amount of mycelium
709 via a sterile toothpick and piercing the media in the center. The assay was performed in triplicate
710 for each isolate used. Cultures were grown at room temperature for 12 days. Siderophore activity

was measured as the area of the plate that has changed to yellow color, when compared to a negative control and an empty petri dish with AY-CAS agar. Pictures of the plates were taken. These images were imported into Adobe Photoshop CC 2019 and size-corrected to 5.5 cm (diameter of the small petri dish). All images were concatenated in the same file. The Color Range tool of Adobe Photoshop CC tool was used to measure the yellow area for all plates. The area measurements were exported into R, where an analysis of variance was performed to determine significant differences across the siderophore activity of the strains.

## Data availability

All additional files included as supplementary materials in this manuscript and custom scripts used for this analysis can be found in the ZyGoLife GitHub repository (https://github.com/zygolife/Basidiobolus_SM_repo).

## Acknowledgments

We would like to thank Dr. Vincent Bruno and Dr. Ashraf S. Ibrahim for kindly sharing the files of the genome annotation, assembly and gene predictions of *B. meristosporus* B9252 and *B. heterosporus* B8920; Dr. Marc Cubeta and Dr. Gregory Bonito for discussions and recommendations for additional experiments regarding siderophore assays and surfactin-like genes; Dr. Gregory Bonito for allowing us to use the unpublished genome sequences of *Mortierella humilis* PMI_1414, *Mortierella sp*. GBAus27b; Dr. Olafur S. Andrésson for allowing us to use the unpublished genome sequences of *Lobaria pulmonaria*; Dr. Paul Dryer for allowing us to use the unpublished genome sequence of *Xanthoria parietina 46-1-SA22*; Dr. Francis Martin and Dr. Pierre Gladieux for allowing us to use the unpublished genome sequence

735 of *Achaetomium strumarium CBS333.67*; Dr. Francis Martin for allowing us to use the
736 unpublished genome sequences of *Boletus edulis V1* and *Amylostereum chailletii DWAch2*; Dr.
737 Marie-Noëlle Rosso for allowing us to use the unpublished genome sequences of
738 *Abortiporus biennis CIRM-BRFM1778;* Dr. Francis Martin and Dr. Gregory Bonito for allowing
739 us to use the unpublished genome sequence of *Atractiellales rhizophila v2.0;* the 1000 Fungal
740 Genomes Project for the use of the dikarya unpublished genomes; and Sabrina Heitmann, Dr. Ed
741 Barge, Dr. Devin Leopold and Dr. Posy Busby for the *Cladosporium sp.* from the *herbarum*
742 species complex PE-07 sample. This work was supported by the National Science Foundation
743 (DEB-1441604 to JWS; DEB-1557110 and DEB-1441715 to JES). The work conducted by the
744 U.S. Department of Energy Joint Genome Institute, a DOE Office of Science User Facility, is
745 supported by the Office of Science of the U.S. Department of Energy under Contract No. DE-
746 AC02-05CH11231. Any opinions, findings, and conclusions or recommendations expressed in
747 this material are those of the author(s) and do not necessarily reflect the views of the National
748 Science Foundation.
749

## References

Altschul, S.F., Madden, T.L., Schäffer, A.A., Zhang, J., Zhang, Z., Miller, W. and Lipman, D.J., 1997. Gapped BLAST and PSI-BLAST: a new generation of protein database search programs. *Nucleic Acids Research*, *25*(17), pp.3389-3402.

Amorós-Moya, D., Bedhomme, S., Hermann, M. and Bravo, I.G., 2010. Evolution in regulatory regions rapidly compensates the cost of nonoptimal codon usage. *Molecular Biology and Evolution*, *27*(9), pp.2141-2151.

Anders, S., Pyl, P.T. and Huber, W., 2015. HTSeq—a Python framework to work with high-throughput sequencing data. *Bioinformatics*, *31*(2), pp.166-169.

Andrews, M. Y., Santelli, C. M., & Duckworth, O. W. 2016. Layer plate CAS assay for the quantitation of siderophore production and determination of exudation patterns for fungi. *Journal of Microbiological Methods*, 121(C), pp. 41–43. http://doi.org/10.1016/j.mimet.2015.12.012

Ahrendt, S.R., Quandt, C.A., Ciobanu, D., Clum, A., Salamov, A., Andreopoulos, B., Cheng, J.F., Woyke, T., Pelin, A., Henrissat, B. and Reynolds, N.K., 2018. Leveraging single-cell genomics to expand the fungal tree of life. *Nature Microbiology*, 3(12), p.1417.

Armaleo, D., Müller, O., Lutzoni, F., Andrésson, Ó.S., Blanc, G., Bode, H.B., Collart, F.R., Dal Grande, F., Dietrich, F., Grigoriev, I.V. and Joneson, S., 2019. The lichen symbiosis re-viewed through the genomes of Cladonia grayi and its algal partner Asterochloris glomerata. *BMC genomics*, 20(1), p.605

771 Baldeweg, F., Warncke, P., Fischer, D. and Gressler, M., 2019. Fungal Biosurfactants
772 from Mortierella alpina. *Organic Letters*, *21*(5), pp.1444-1448.

773 Bletz, M.C., Goedbloed, D.J., Sanchez, E., Reinhardt, T., Tebbe, C.C., Bhuju, S., Geffers,
774 R., Jarek, M., Vences, M. and Steinfartz, S., 2016. Amphibian gut microbiota shifts differentially
775 in community structure but converges on habitat-specific predicted functions. *Nature*
776 *Communications*, *7*, p.13699.

777 Blin, K., Wolf, T., Chevrette, M.G., Lu, X., Schwalen, C.J., Kautsar, S.A., Suarez Duran,
778 H.G., de Los Santos, E.L., Kim, H.U., Nave, M. and Dickschat, J.S., 2017. antiSMASH 4.0—
779 improvements in chemistry prediction and gene cluster boundary identification. *Nucleic Acids*
780 *Research*, *45*(W1), pp.W36-W41.

781 Brakhage, A.A., 2013. Regulation of fungal secondary metabolism. *Nature Reviews*
782 *Microbiology*, *11*(1), p.21.

783 Braun V., Hantke K. (2013) The Tricky Ways Bacteria Cope with Iron Limitation. In:
784 Chakraborty R., Braun V., Hantke K., Cornelis P. (eds) Iron Uptake in Bacteria with Emphasis
785 on E. coli and Pseudomonas. SpringerBriefs in Molecular Science. Springer, Dordrecht

786 Burmester, A., Richter, M., Schultze, K., Voelz, K., Schachtschabel, D., Boland, W.,
787 Wöstemeyer, J. and Schimek, C., 2007. Cleavage of β-carotene as the first step in sexual
788 hormone synthesis in zygomycetes is mediated by a trisporic acid regulated β-carotene
789 oxygenase. *Fungal Genetics and Biology*, *44*(11), pp.1096-1108.

790 Burmester, A., Shelest, E., Glöckner, G., Heddergott, C., Schindler, S., Staib, P., Heidel,
791 A., Felder, M., Petzold, A., Szafranski, K. and Feuermann, M., 2011. Comparative and

792 functional genomics provide insights into the pathogenicity of dermatophytic fungi. *Genome*
793 *biology*, 12(1), p.R7

794 Bushley, K.E. and Turgeon, B.G., 2010. Phylogenomics reveals subfamilies of fungal
795 nonribosomal peptide synthetases and their evolutionary relationships. *BMC Evolutionary*
796 *Biology*, *10*(1), p.26.

797 Bushley, K.E., Raja, R., Jaiswal, P., Cumbie, J.S., Nonogaki, M., Boyd, A.E., Owensby,
798 C.A., Knaus, B.J., Elser, J., Miller, D. and Di, Y., 2013. The genome of *Tolypocladium inflatum:*
799 evolution, organization, and expression of the cyclosporin biosynthetic gene cluster. *PLoS*
800 *genetics*, 9(6).

801 Capella-Gutiérrez, S., Silla-Martínez, J.M. and Gabaldón, T., 2009. trimAl: a tool for
802 automated alignment trimming in large-scale phylogenetic analyses. *Bioinformatics*, *25*(15),
803 pp.1972-1973.

804 Chang, Y., Wang, S., Sekimoto, S., Aerts, A.L., Choi, C., Clum, A., LaButti, K.M.,
805 Lindquist, E.A., Yee, Ngan C., Ohm, R.A., Salamov, A.A., Grigoriev, I.V., Spatafora, J.W., and
806 Berbee M.L. 2015. Phylogenomic Analyses Indicate that Early Fungi Evolved Digesting Cell
807 Walls of Algal Ancestors of Land Plants. *Genome Biology and Evolution*, 14;7(6):1590-601. doi:
808 10.1093/gbe/evv090.

809 Chang, Y., Desirò, A., Na, H., Sandor, L., Lipzen, A., Clum, A., Barry, K., Grigoriev,
810 I.V., Martin, F.M., Stajich, J.E. and Smith, M.E., 2019. Phylogenomics of Endogonaceae and
811 evolution of mycorrhizas within Mucoromycota. *New Phytologist*, 222(1), pp.511-525.

812 Charif, D. and Lobry, J.R., 2007. SeqinR 1.0-2: a contributed package to the R project for
813 statistical computing devoted to biological sequences retrieval and analysis. In Structural
814 approaches to sequence evolution (pp. 207-232). Springer, Berlin, Heidelberg.

815 Chen, E.C.H., Morin, E., Beaudet, D., Noel, J., Yildirir, G., Ndikumana, S., Charron, P.,
816 St-Onge, C., Giorgi J., Kruger, M., Marton, T., Ropars, J., Grigoriev, I.V., Hainaut, M.,
817 Henrissat, B., Roux, C., Martin, F. and Corradi, N. 2018. High intraspecific genome diversity in
818 the model arbuscular mycorrhizal symbiont Rhizophagus irregularis. *New Phytologist*,
819 220(4):1161-1171. doi: 10.1111/nph.14989.

820 Chibucos, M.C., Soliman, S., Gebremariam, T., Lee, H., Daugherty, S., Orvis, J., Shetty,
821 A.C., Crabtree, J., Hazen, T.H., Etienne, K.A. and Kumari, P., 2016. An integrated genomic and
822 transcriptomic survey of mucormycosis-causing fungi. *Nature Communications*, *7*, p.12218.

823 Collemare, J., Pianfetti, M., Houlle, A.E., Morin, D., Camborde, L., Gagey, M.J.,
824 Barbisan, C., Fudal, I., Lebrun, M.H. and Böhnert, H.U., 2008. Magnaporthe grisea avirulence
825 gene ACE1 belongs to an infection□specific gene cluster involved in secondary metabolism.
826 *New Phytologist*, *179*(1), pp.196-208.

827 Colston, T.J. and Jackson, C.R., 2016. Microbiome evolution along divergent branches of
828 the vertebrate tree of life: what is known and unknown. *Molecular Ecology*, *25*(16), pp.3776-
829 3800.

830 Corrochano, L.M., Kuo, A., Marcet-Houben, M., Polaino, S., Salamov, A., Villalobos-
831 Escobedo, J.M., Grimwood, J., Alvarez, M.I., Avalos, J., Bauer, D., Benito, E.P., Benoit, I.,
832 Burger, G., Camino, L.P., Canovas, D., Cerda-Olmedo, E., Cheng, J.F., Dominguez, A., Elias,
833 M., Eslava, AP., Glaser, F., Gutierrez, G., Heitman, J., Henrissat, B., Iturriaga, E.A., Lang, B.F.,

834 Lavin, J.L., Lee, S.C., Li, W., Lindquist, E., Lopez-Garcia, S., Luque, E.M., Marcos, A.T.,
835 Martin, J., McCluskey, K., Medina, H.R., Miralles-Duran, A., Miyazaki, A., Munoz-Torres, E.,
836 Oguiza, J.A., Ohm, R.A., Olmedo, M., Oreja,s M., Ortiz-Castellanos, L., Pisabarro, A.G.,
837 Rodriguez-Romero, J., Ruiz-Herrera, J., Ruiz-Vazquez, R., Sanz, C., Schackwitz, W., Shahriari,
838 M., Shelest, E., Silva-Franco, F., Soanes, D., Syed, K., Tagua, V.G., Talbot, N.J., Thon, M.R.,
839 Tice, H., de Vries, R.P., Wiebenga, A., Yadav, J.S., Braun, E.L., Baker, S,E., Garre, V.,
840 Schmutz, J., Horwitz, B.A., Torres-Martinez, S., Idnurm, A., Herrera-Estrella, A., Gabaldon and
841 T., Grigoriev, I.V. 2016. Expansion of Signal Transduction Pathways in Fungi by Extensive
842 Genome Duplication. *Current Biology*, 26(12):1577-1584. doi: 10.1016/j.cub.2016.04.038.

843 Costello, E.K., Gordon, J.I., Secor, S.M. and Knight, R., 2010. Postprandial remodeling
844 of the gut microbiota in Burmese pythons. *The ISME journal*, *4*(11), p.1375.

845 Da Lage, J.L., Binder, M., Hua-Van, A., Janeček, Š. and Casane, D., 2013. Gene make-
846 up: rapid and massive intron gains after horizontal transfer of a bacterial α-amylase gene to
847 Basidiomycetes. *BMC evolutionary biology*, 13(1), p.40.

848 DiGuistini, S., Wang, Y., Liao, N.Y., Taylor, G., Tanguay, P., Feau, N., Henrissat, B.,
849 Chan, S.K., Hesse-Orce, U., Alamouti, S.M. and Tsui, C.K., 2011. Genome and transcriptome
850 analyses of the mountain pine beetle-fungal symbiont Grosmannia clavigera, a lodgepole pine
851 pathogen. *Proceedings of the National Academy of Sciences*, 108(6), pp.2504-2509.

852 Dimkpa, C., 2016. Microbial siderophores: Production, detection and application in
853 agriculture and environment. *Endocytobiosis & Cell Research*, *27*(2), pp. 7-16

854 Eddy, S.R., 2004. What is a hidden Markov model?. *Nature Biotechnology*, *22*(10),
855 p.1315.

Emms, D.M. and Kelly, S., 2015. OrthoFinder: solving fundamental biases in whole genome comparisons dramatically improves orthogroup inference accuracy. *Genome Biology*, *16*(1), p.157.

Finn, R.D., Mistry, J., Tate, J., Coggill, P., Heger, A., Pollington, J.E., Gavin, O.L., Gunasekaran, P., Ceric, G., Forslund, K. and Holm, L., 2009. The Pfam protein families database. *Nucleic Acids Research*, *38*(suppl_1), pp.D211-D222.

Floudas, D., Binder, M., Riley, R., Barry, K., Blanchette, R.A., Henrissat, B., Martínez, A.T., Otillar, R., Spatafora, J.W., Yadav, J.S. and Aerts, A., 2012. The Paleozoic origin of enzymatic lignin decomposition reconstructed from 31 fungal genomes. *Science*, 336(6089), pp.1715-1719.

Ffrench-Constant, R.H., Waterfield, N., Burland, V., Perna, N.T., Daborn, P.J., Bowen, D. and Blattner, F.R., 2000. A genomic sample sequence of the entomopathogenic bacterium Photorhabdus luminescens W14: potential implications for virulence. *Applied Environmental Microbiology*, *66*(8), pp.3310-3329.

Gaillard DL (2014) Population genetics and microbial communities of the Gopher Tortoise (Gopherus polyphemus). Unpublished MS Thesis, The University of Southern Mississippi.

Gawad, C., Koh, W. and Quake, S.R., 2016. Single-cell genome sequencing: current state of the science. *Nature Reviews Genetics*, *17*(3), p.175.

Gostinčar, C., Ohm, R.A., Kogej, T., Sonjak, S., Turk, M., Zajc, J., Zalar, P., Grube, M., Sun, H., Han, J. and Sharma, A., 2014. Genome sequencing of four Aureobasidium pullulans

varieties: biotechnological potential, stress tolerance, and description of new species. *BMC genomics*, 15(1), p.549.

Grigoriev IV, Nikitin R, Haridas S, Kuo A, Ohm R, Otillar R, Riley R, Salamov A, Zhao X, Korzeniewski F, Smirnova T, Nordberg H, Dubchak I, Shabalov I., 2014. MycoCosm portal: gearing up for 1000 fungal genomes. Nucleic Acids Res. 42(1):D699-704.

Haridas, S., Albert, R., Binder, M., Bloem, J., LaButti, K., Salamov, A., Andreopoulos, B., Baker, S.E., Barry, K., Bills, G. and Bluhm, B.H., 2020. 101 Dothideomycetes genomes: a test case for predicting lifestyles and emergence of pathogens. *Studies in Mycology*. https://doi.org/10.1016/j.simyco.2020.01.003

Helaly, S.E., Thongbai, B. and Stadler, M., 2018. Diversity of biologically active secondary metabolites from endophytic and saprotrophic fungi of the ascomycete order Xylariales. *Natural Product Reports*, *35*(9), pp.992-1014.

Hong, P.Y., Wheeler, E., Cann, I.K. and Mackie, R.I., 2011. Phylogenetic analysis of the fecal microbial community in herbivorous land and marine iguanas of the Galápagos Islands using 16S rRNA-based pyrosequencing. *The ISME journal*, *5*(9), p.1461.

Katoh, K., Rozewicki, J. and Yamada, K.D., 2017. MAFFT online service: multiple sequence alignment, interactive sequence choice and visualization. *Briefings in Bioinformatics*.

Karlsson, M., Atanasova, L., Jensen, D.F. and Zeilinger, S., 2016. Necrotrophic mycoparasites and their genomes. *Spectrum*, *5*(2).

Keller, N.P., Turner, G. and Bennett, J.W., 2005. Fungal secondary metabolism—from biochemistry to genomics. *Nature Reviews Microbiology*, *3*(12), p.937.

898 Khaldi, N., Seifuddin, F.T., Turner, G., Haft, D., Nierman, W.C., Wolfe, K.H. and
899 Fedorova, N.D., 2010. SMURF: genomic mapping of fungal secondary metabolite clusters.
900 *Fungal Genetics and Biology*, *47*(9), pp.736-741.

901 Kohl, K.D., Cary, T.L., Karasov, W.H. and Dearing, M.D., 2013. Restructuring of the
902 amphibian gut microbiota through metamorphosis. *Environmental Microbiology Reports*, *5*(6),
903 pp.899-903.

904 Kohler, A., Kuo, A., Nagy, L.G., Morin, E., Barry, K.W., Buscot, F., Canbäck, B., Choi,
905 C., Cichocki, N., Clum, A. and Colpaert, J., 2015. Convergent losses of decay mechanisms and
906 rapid turnover of symbiosis genes in mycorrhizal mutualists. *Nature Genetics*, *47*(4), p.410.

907 Kroken, S., Glass, N.L., Taylor, J.W., Yoder, O.C. and Turgeon, B.G., 2003.
908 Phylogenomic analysis of type I polyketide synthase genes in pathogenic and saprobic
909 ascomycetes. *Proceedings of the National Academy of Sciences*, *100*(26), pp.15670-15675.

910 Lawrence, M., Huber, W., Pages, H., Aboyoun, P., Carlson, M., Gentleman, R., Morgan,
911 M.T. and Carey, V.J., 2013. Software for computing and annotating genomic ranges. *PLoS*
912 *Computational Biology*, 9(8), p.e1003118.

913 Lastovetsky, O.A., Gaspar, M.L., Mondo, S.J., LaButti, K.M., Sandor, L., Grigoriev, IV.,
914 Henry, S.A. and Pawlowska, T.E. 2016. Lipid metabolic changes in an early divergent fungus
915 govern the establishment of a mutualistic symbiosis with endobacteria. *Proceedings of the*
916 *National Academy of Sciences*, 113(52):15102-15107. doi: 10.1073/pnas.1615148113.

917 Li, H. and Durbin, R., 2009. Fast and accurate short read alignment with Burrows–
918 Wheeler transform. *Bioinformatics*, *25*(14), pp.1754-1760.

Li, H., Handsaker, B., Wysoker, A., Fennell, T., Ruan, J., Homer, N., Marth, G., Abecasis, G. and Durbin, R., 2009. The sequence alignment/map format and SAMtools. *Bioinformatics*, *25*(16), pp.2078-2079.

Luo, H., Hong, S.Y., Sgambelluri, R.M., Angelos, E., Li, X. and Walton, J.D., 2014. Peptide macrocyclization catalyzed by a prolyl oligopeptidase involved in α-amanitin biosynthesis. *Chemistry & Biology*, *21*(12), pp.1610-1617.

Ma, L.J., Ibrahim, A.S., Skory, C., Grabherr, M.G., Burger, G., Butler, M., Elias, M., Idnurm, A., Lang, B.F., Sone, T., Abe, A., Calvo, S.E., Corrochano, L.M., Engels, R., Fu, J., Hansberg, W., Kim, J.M., Kodira, C.D., Koehrsen, M.J., Liu, B., Miranda-Saavedra, D., O'Leary, S., Ortiz-Castellanos, L., Poulter, R., Rodriguez-Romero, J., Ruiz-Herrera, J., Shen, Y.Q., Zeng, Q., Galagan, J., Birren, B.W., Cuomo, C.A. and Wickes B.L. 2009. Genomic analysis of the basal lineage fungus Rhizopus oryzae reveals a whole-genome duplication. *PLoS Genetics*, 5(7):e1000549. doi: 10.1371/journal.pgen.1000549.

Martino, E., Morin, E., Grelet, G.A., Kuo, A., Kohler, A., Daghino, S., Barry, K.W., Cichocki, N., Clum, A., Dockter, R.B. and Hainaut, M., 2018. Comparative genomics and transcriptomics depict ericoid mycorrhizal fungi as versatile saprotrophs and plant mutualists. *New Phytologist*, 217(3), pp.1213-1229.

Medrano-Soto, A., Moreno-Hagelsieb, G., Vinuesa, P., Christen, J.A. and Collado-Vides, J., 2004. Successful lateral transfer requires codon usage compatibility between foreign genes and recipient genomes. *Molecular Biology and Evolution*, *21*(10), pp.1884-1894.

939 Mondo, S.J., Dannebaum, R.O., Kuo, R.C., Louie, K.B., Bewick, A.J., LaButti, K.,
940 Haridas, S., Kuo, A., Salamov, A., Ahrendt, S.R. and Lau, R., 2017. Widespread adenine N6-
941 methylation of active genes in fungi. *Nature Genetics*, *49*(6), p.964.

942 Morin, E., Kohler, A., Baker, A.R., Foulongne-Oriol, M., Lombard, V., Nagye, L.G.,
943 Ohm, R.A., Patyshakuliyeva, A., Brun, A., Aerts, A.L. and Bailey, A.M., 2012. Genome
944 sequence of the button mushroom Agaricus bisporus reveals mechanisms governing adaptation
945 to a humic-rich ecological niche. *Proceedings of the National Academy of Sciences*, 109(43),
946 pp.17501-17506.

947 Murphy, C., Youssef, N., Hanafy, R.A., Couger, M.B., Stajich, J.E., Wang, Y., Baker, K.,
948 Dagar, S., Griffith, G., Farag, I. and Callaghan, T.M., 2019. Horizontal gene transfer as an
949 indispensible driver for Neocallimastigomycota evolution into a distinct gut-dwelling fungal
950 lineage. *bioRxiv*, p.487215.

951 Nagy, G., Farkas, A., Csernetics, Á., Bencsik, O., Szekeres, A., Nyilasi, I., Vágvölgyi, C.
952 and Papp, T., 2014. Transcription of the three HMG-CoA reductase genes of Mucor
953 circinelloides. *BMC Microbiology*, *14*(1), p.93.

954 Nagy, L.G., Riley, R., Tritt, A., Adam, C., Daum, C., Floudas, D., Sun, H., Yadav, J.S.,
955 Pangilinan, J., Larsson, K.H. and Matsuura, K., 2016. Comparative genomics of early-diverging
956 mushroom-forming fungi provides insights into the origins of lignocellulose decay capabilities.
957 *Molecular Biology and Evolution*, 33(4), pp.959-970.

958 Nguyen, T.A., Cissé, O.H., Wong, J.Y., Zheng, P., Hewitt, D., Nowrousian, M., Stajich,
959 J.E. and Jedd, G., 2017. Innovation and constraint leading to complex multicellularity in the
960 Ascomycota. *Nature communications*, 8(1), pp.1-13.

961 Ohm, R.A., Feau, N., Henrissat, B., Schoch, C.L., Horwitz, B.A., Barry, K.W., Condon,
962 B.J., Copeland, A.C., Dhillon, B., Glaser, F. and Hesse, C.N., 2012. Diverse lifestyles and
963 strategies of plant pathogenesis encoded in the genomes of eighteen Dothideomycetes fungi.
964 *PLoS Pathogens*, 8(12).

965 Okagaki, L.H., Nunes, C.C., Sailsbery, J., Clay, B., Brown, D., John, T., Oh, Y., Young,
966 N., Fitzgerald, M., Haas, B.J. and Zeng, Q., 2015. Genome sequences of three phytopathogenic
967 species of the Magnaporthaceae family of fungi. *G3: Genes, Genomes, Genetics*, 5(12), pp.2539-
968 2545.

969 O'Leary, N.A., Wright, M.W., Brister, J.R., Ciufo, S., Haddad, D., McVeigh, R., Rajput,
970 B., Robbertse, B., Smith-White, B., Ako-Adjei, D. and Astashyn, A., 2015. Reference sequence
971 (RefSeq) database at NCBI: current status, taxonomic expansion, and functional annotation.
972 *Nucleic Acids Research*, *44*(D1), pp.D733-D745.

973 Osbourn, A., 2010. Gene clusters for secondary metabolic pathways: an emerging theme
974 in plant biology. *Plant Physiology*, *154*(2), pp.531-535.

975 Pagès, H., Aboyoun, P., Gentleman, R. and DebRoy, R. 2019. Biostrings: Efficient
976 manipulation of biological strings. R package version 2.52.0.

977 Padamsee, M., Kumar, T.A., Riley, R., Binder, M., Boyd, A., Calvo, A.M., Furukawa,
978 K., Hesse, C., Hohmann, S., James, T.Y. and LaButti, K., 2012. The genome of the xerotolerant
979 mold Wallemia sebi reveals adaptations to osmotic stress and suggests cryptic sexual
980 reproduction. *Fungal Genetics and Biology*, 49(3), pp.217-226.

981 Paterson, R.R.M., 2008. Cordyceps–a traditional Chinese medicine and another fungal
982 therapeutic biofactory?. *Phytochemistry*, *69*(7), pp.1469-1495.

983 Pendleton, A.L., Smith, K.E., Feau, N., Martin, F.M., Grigoriev, I.V., Hamelin, R.,
984 Nelson, C.D., Burleigh, J.G. and Davis, J.M., 2014. Duplications and losses in gene families of
985 rust pathogens highlight putative effectors. *Frontiers in plant science*, 5, p.299.

986 Peypoux, F., Bonmatin, J.M. and Wallach, J., 1999. Recent trends in the biochemistry of
987 surfactin. *Applied Microbiology and Biotechnology*, 51(5), pp.553-563.

988 Pusztahelyi, T., Holb, I.J. and Pócsi, I., 2015. Secondary metabolites in fungus-plant
989 interactions. *Frontiers in Plant Science*, *6*, p.573.

990 Quandt, C.A., Beaudet, D., Corsaro, D., Walochnik, J., Michel, R., Corradi, N. and
991 James, T.Y., 2017. The genome of an intranuclear parasite, Paramicrosporidium saccamoebae,
992 reveals alternative adaptations to obligate intracellular parasitism. *Elife*, *6*, p.e29594.

993 Reynolds, H.T., Vijayakumar, V., Gluck□Thaler, E., Korotkin, H.B., Matheny, P.B. and
994 Slot, J.C., 2018. Horizontal gene cluster transfer increased hallucinogenic mushroom diversity.
995 *Evolution Letters*, *2*(2), pp.88-101.

996 Robinson, M.D., McCarthy, D.J., and Smyth, G.K. 2010. edgeR: a Bioconductor
997 package for differential expression analysis of digital gene expression data. *Bioinformatics* 26,
998 139-140

999 Rokas, A., Mead, M. E., Steenwyk, J. L., Raja, H. A., & Oberlies, N. H. 2020.
1000 Biosynthetic gene clusters and the evolution of fungal chemodiversity. *Natural Product Reports*
1001 17, pp. 167-178. http://doi.org/10.1039/c9np00045c

1002 Riley, R., Salamov, A.A., Brown, D.W., Nagy, L.G., Floudas, D., Held, B.W., Levasseur,
1003 A., Lombard, V., Morin, E., Otillar, R. and Lindquist, E.A., 2014. Extensive sampling of

basidiomycete genomes demonstrates inadequacy of the white-rot/brown-rot paradigm for wood decay fungi. *Proceedings of the National Academy of Sciences*, 111(27), pp.9923-9928.

Schwartze, V.U., Winter, S., Shelest, E., Marcet-Houben, M., Horn, F., Wehner, S., Linde, J., Valiante, V., Sammeth, M., Riege, K., Nowrousian, M., Kaerger, K., Jacobsen, I.D., Marz, M., Brakhage, A.A., Gabaldon, T., Bocker, S. and Voigt, K. 2014. Gene expansion shapes genome architecture in the human pathogen Lichtheimia corymbifera: an evolutionary genomics analysis in the ancient terrestrial mucorales (Mucoromycotina). *PLoS Genetics*, 10(8):e1004496. doi: 10.1371/journal.pgen.1004496.

Smith, D.J., Burnham, M.K., Edwards, J., Earl, A.J. and Turner, G., 1990. Cloning and heterologous expression of the penicillin biosynthetic gene cluster from Penicillium chrysogenum. *Bio/technology*, *8*(1), p.39.

Spatafora, J.W., Chang, Y., Benny, G.L., Lazarus, K., Smith, M.E., Berbee, M.L., Bonito, G., Corradi, N., Grigoriev, I., Gryganskyi, A. and James, T.Y., 2016. A phylum-level phylogenetic classification of zygomycete fungi based on genome-scale data. *Mycologia*, *108*(5), pp.1028-1046.

Stamatakis, A., 2014. RAxML version 8: a tool for phylogenetic analysis and post-analysis of large phylogenies. *Bioinformatics*, *30*(9), pp.1312-1313.

Team, R.C., 2018. R: A language and environment for statistical computing.

Teixeira, M.D.M., Moreno, L.F., Stielow, B.J., Muszewska, A., Hainaut, M., Gonzaga, L., Abouelleil, A., Patané, J.S.L., Priest, M., Souza, R. and Young, S., 2017. Exploring the

genomic diversity of black yeasts and relatives (Chaetothyriales, Ascomycota). *Studies in mycology*, 86, pp.1-28.

Terfehr, D., Dahlmann, T.A., Specht, T., Zadra, I., Kürnsteiner, H. and Kück, U., 2014. Genome sequence and annotation of Acremonium chrysogenum, producer of the β-lactam antibiotic cephalosporin C. *Genome Announcements*, 2(5), pp.e00948-14.

Tisserant, E., Malbreil, M., Kuo, A., Kohler, A., Symeonidi, A., Balestrini, R., Charron, P., Duensing, N., Frei dit Frey, N., Gianinazzi-Pearson, V., Gilbert, L.B., Handa, Y., Herr, J.R., Hijri, M., Koul, R., Kawaguchi, M., Krajinski, F., Lammers, P.J., Masclaux, F.G., Murat, C., Morin, E., Ndikumana, S., Pagni, M., Petitpierre, D., Requena, N., Rosikiewicz, P., Riley, R., Saito, K., San Clemente, H., Shapiro, H., van Tuinen, D., Becard, G., Bonfante, P., Paszkowski, U., Shachar-Hill, Y.Y., Tuskan, G.A., Young, J.P., Sanders, I.R., Henrissat, B., Rensing, S.A., Grigoriev, I.V., Corradi, N., Roux, C. and Martin, F. 2013. Genome of an arbuscular mycorrhizal fungus provides insight into the oldest plant symbiosis. *Proceedings of the National Academy of Sciences*, 10;110(50):20117-22. doi: 10.1073/pnas.1313452110.

Tuller, T. 2011. Codon bias, tRNA pools, and horizontal gene transfer. *Mobile Genetic Elements, 1(1),* pp. 75-77, DOI: 10.4161/mge.1.1.15400

Uehling, J., Gryganskyi, A., Hameed, K., Tschaplinski, T., Misztal, PK., Wu S., Desiro, A., Vande Pol, N., Du, Z., Zienkiewicz, A., Zienkiewicz, K., Morin, E., Tisserant, E., Splivallo, R., Hainaut, M., Henrissat, B., Ohm, R., Kuo, A., Yan, J., Lipzen, A., Nolan, M., LaButti, K., Barry, K., Goldstein, A.H., Labbe, J., Schadt, C., Tuskan, G., Grigoriev, I., Martin, F., Vilgalys, R. and Bonito, G. 2017. Comparative genomics of Mortierella elongata and its bacterial endosymbiont Mycoavidus cysteinexigens. 2017. *Environmental Microbiology*, 19(8):2964-2983. doi: 10.1111/1462-2920.13669

1048 Vesth, T.C., Nybo, J.L., Theobald, S., Frisvad, J.C., Larsen, T.O., Nielsen, K.F., Hoof,
1049 J.B., Brandl, J., Salamov, A., Riley, R. and Gladden, J.M., 2018. Investigation of inter-and
1050 intraspecies variation through genome sequencing of Aspergillus section Nigri. *Nature Genetics*,
1051 50(12), pp.1688-1695.

1052 Voigt, K., Wolf, T., Ochsenreiter, K., Nagy, G., Kaerger, K., Shelest, E. and Papp, T.,
1053 2016. 15 Genetic and Metabolic Aspects of Primary and Secondary Metabolism of the
1054 Zygomycetes. In *Biochemistry and Molecular Biology* (pp. 361-385). Springer, Cham.

1055 Wisecaver, J.H. and Rokas, A., 2015. Fungal metabolic gene clusters—caravans traveling
1056 across genomes and environments. *Frontiers in Microbiology*, 6, p.161.

1057 Wang, D., Wu, R., Xu, Y. and Li, M. 2013. Draft Genome Sequence of Rhizopus
1058 chinensis CCTCCM201021., Used for Brewing Traditional Chinese Alcoholic Beverages.
1059 *Genome Announcements*, 1(2):e0019512. doi: 10.1128/genomeA.00195-12.

1060 Wang, Y., White, M.M., Kvist, S. and Moncalvo, J.M. 2016. Genome-Wide Survey of
1061 Gut Fungi (Harpellales) Reveals the First Horizontally Transferred Ubiquitin Gene from a
1062 Mosquito Host. *Molecular Biology and Evolution*, 33(10):2544-54. doi:
1063 10.1093/molbev/msw126.

1064 Wang, Y., Youssef, N., Couger, M.B., Hanafy, R., Elshahed, M. and Stajich, J.E., 2018.
1065 Comparative genomics and divergence time estimation of the anaerobic fungi in herbivorous
1066 mammals. *bioRxiv*, p.401869.

1067 Wang, Y.Y., Liu, B., Zhang, X.Y., Zhou, Q.M., Zhang, T., Li, H., Yu, Y.F., Zhang, X.L.,
1068 Hao, X.Y., Wang, M. and Wang, L., 2014. Genome characteristics reveal the impact of

1069 lichenization on lichen-forming fungus Endocarpon pusillum Hedwig (Verrucariales,
1070 Ascomycota). *BMC Genomics*, 15(1), p.34.

1071 Wickham, H. 2016. ggplot2: Elegant Graphics for Data Analysis. Springer-Verlag New
1072 York.

1073 Winter, D.J., 2017. rentrez: An R package for the NCBI eUtils API (No. e3179v1). *PeerJ*
1074 *Preprints.*

1075 Xiao, J.H. and Zhong, J.J., 2007. Secondary metabolites from Cordyceps species and
1076 their antitumor activity studies. *Recent Patents on Biotechnology*, *1*(2), pp.123-137.

1077 Xiao, G., Ying, S.H., Zheng, P., Wang, Z.L., Zhang, S., Xie, X.Q., Shang, Y., Leger,
1078 R.J.S., Zhao, G.P., Wang, C. and Feng, M.G., 2012. Genomic perspectives on the evolution of
1079 fungal entomopathogenicity in Beauveria bassiana. *Scientific reports*, 2, p.483.

1080 Yang, J., Wang, L., Ji, X., Feng, Y., Li, X., Zou, C., Xu, J., Ren, Y., Mi, Q., Wu, J. and
1081 Liu, S., 2011. Genomic and proteomic analyses of the fungus Arthrobotrys oligospora provide
1082 insights into nematode-trap formation. *PLoS pathogens*, 7(9).

1083 Zhang, X.Y., Bao, J., Wang, G.H., He, F., Xu, X.Y. and Qi, S.H., 2012. Diversity and
1084 antimicrobial activity of culturable fungi isolated from six species of the South China Sea
1085 gorgonians. *Microbial Ecology*, *64*(3), pp.617-627.

1086 Zuccaro, A., Lahrmann, U., Gueldener, U., Langen, G., Pfiffi, S., Biedenkopf, D., Wong,
1087 P., Samans, B., Grimm, C., Basiewicz, M. and Murat, C., 2011. Endophytic life strategies
1088 decoded by genome and transcriptome analyses of the mutualistic root symbiont Piriformospora
1089 indica. *PLoS pathogens*, 7(10).

1090

1091

# Tables

**Table 1.** Predicted secondary metabolite (SM) core genes for *Basidiobolus* isolates used in this study. NRPS: Non-ribosomal peptide synthetases, PKS: Polyketide synthases, TC: Terpene cyclases.

| Isolate | Total SM | NRPS/NRPS-like | PKS/PKS-Like | NRPS-PKS hybrids | TC |
|---|---|---|---|---|---|
| *B. meristosporus* CBS 931.73 | 44 | 30 | 4 | 0 | 10 |
| *B. meristosporus* B9252 | 43 | 29 | 7 | 1 | 6 |
| *B. heterosporus* B8920 | 23 | 18 | 1 | 0 | 4 |

**Table 2.** Number of predicted secondary metabolite core genes with evidence for HGI in *Basidiobolus* genomes. NRPS: Non-ribosomal peptide synthetases, PKS: Polyketide synthases, TC: Terpene cyclases.

| Isolate | Total SM | NRPS/NRPS-like | PKS/PKS-Like | NRPS-PKS hybrids | TC |
|---|---|---|---|---|---|
| *B. meristosporus* CBS 931.73 | 26/44 (61%) | 22/30 (60%) | 2/4 (50%) | 0/0 (0%) | 2/10 (2%) |
| *B. meristosporus* B9252 | 19/43 (44%) | 16/29 (55%) | 1/7 (14%) | 0/1 (0%) | 2/6 (1.4%) |
| *B. heterosporus* B8920 | 12/23 (52%) | 12/18 (66%) | 0/1 (0%) | 0/0 (0%) | 0/4 (0%) |

**Table 3.** Summary of secondary metabolite core genes with HGT evidence from *Basidiobolus* isolates.

| Isolate | Gene | Z-score of gene coverage | SM class | Taxonomy for best NCBI hit |
|---|---|---|---|---|
| *B. heterosporus* | N168_02885 | -0.104 | NRPS | b-proteobacteria |
| | N168_00992 | 0.028 | NRPS | enterobacteria |
| | N168_05934 | -0.183 | NRPS | b-proteobacteria |
| | N168_07140 | 0.260 | NRPS | b-proteobacteria |
| | N168_06479 | 0.328 | NRPS | b-proteobacteria |
| | N168_00176 | 0.013 | NRPS | cyanobacteria |
| | N168_08721 | 0.561 | NRPS | cyanobacteria |
| | N168_05966 | 0.672 | NRPS | d-proteobacteria |
| | N168_05324 | -0.038 | NRPS-Like | cyanobacteria |
| | N168_08580 | 0.047 | NRPS-Like | d-proteobacteria |
| | N168_03036 | 0.022 | NRPS-Like | d-proteobacteria |
| | N168_04239 | 0.070 | NRPS-Like | b-proteobacteria |
| *B. meristosporus B9252* | N161.mRNA.1431.1 | -0.350 | NRPS | cyanobacteria |
| | N161.mRNA.1485.1 | -0.258 | NRPS | d-proteobacteria |
| | N161.mRNA.2152.1 | 0.074 | NRPS | cyanobacteria |
| | N161.mRNA.4115.1 | 0.158 | NRPS | enterobacteria |
| | N161.mRNA.4211.1 | 0.243 | NRPS | cyanobacteria |
| | N161.mRNA.4324.1 | 0.213 | NRPS | CFB group bacteria |
| | N161.mRNA.8304.1 | 0.358 | NRPS | b-proteobacteria |
| | N161.mRNA.9145.1 | 0.201 | NRPS | cyanobacteria |
| | N161.mRNA.9317.1 | 0.677 | NRPS | d-proteobacteria |
| | N161.mRNA.9639.1 | -0.151 | NRPS | d-proteobacteria |
| | N161.mRNA.11289.1 | 0.596 | NRPS | cyanobacteria |
| | N161.mRNA.1486.1 | 0.662 | NRPS-Like | firmicutes |
| | N161.mRNA.5862.1 | 1.131 | NRPS-Like | firmicutes |
| | N161.mRNA.6846.1 | 0.760 | NRPS-Like | firmicutes |
| | N161.mRNA.6935.1 | 0.624 | NRPS-Like | d-proteobacteria |
| | N161.mRNA.8699.1 | -0.201 | NRPS-Like | firmicutes |
| | N161.mRNA.6146.1 | 0.999 | PKS | high GC Gram+ |
| | N161.mRNA.1413.1 | 0.481 | Terpene | CFB group bacteria |
| | N161.mRNA.13969.1 | 1.099 | Terpene | CFB group bacteria |

| | | | | |
|---|---|---|---|---|
| | 366903 | 0.043 | NRPS | a-proteobacteria |
| | 368581 | -0.232 | NRPS | b-proteobacteria |
| | 349800 | 0.208 | NRPS | high GC Gram+ |
| | 351909 | -0.120 | NRPS | cyanobacteria |
| | 372749 | -0.088 | NRPS | firmicutes |
| | 372991 | -0.260 | NRPS | b-proteobacteria |
| | 373247 | 0.533 | NRPS | firmicutes |
| | 373940 | -0.142 | NRPS | firmicutes |
| | 375475 | 0.522 | NRPS | enterobacteria |
| | 338397 | 0.033 | NRPS | d-proteobacteria |
| | 375580 | 0.033 | NRPS | cyanobacteria |
| | 375613 | -0.369 | NRPS | firmicutes |
| | 377413 | -0.245 | NRPS | g-proteobacteria |
| | 387529 | -0.157 | NRPS | b-proteobacteria |
| | 307892 | 0.404 | NRPS | a-proteobacteria |
| *B. meristosporus CBS 931.73* | 298977 | -0.201 | NRPS | b-proteobacteria |
| | 343011 | 0.147 | NRPS | firmicutes |
| | 363930 | -0.358 | NRPS | firmicutes |
| | 300898 | -0.165 | NRPS-Like | firmicutes |
| | 322666 | -0.174 | NRPS-Like | CFB group bacteria |
| | 146993 | -0.200 | NRPS-Like | cyanobacteria |
| | 382467 | -0.264 | NRPS-Like | a-proteobacteria |
| | 340613 | -0.136 | NRPS-Like | GNS bacteria |
| | 237744 | -0.001 | PKS | bacteria |
| | 292783 | -0.429 | PKS | high GC Gram+ |
| | 301341 | -0.210 | Terpene | CFB group bacteria |
| | 304520 | 0.389 | Terpene | cyanobacteria |

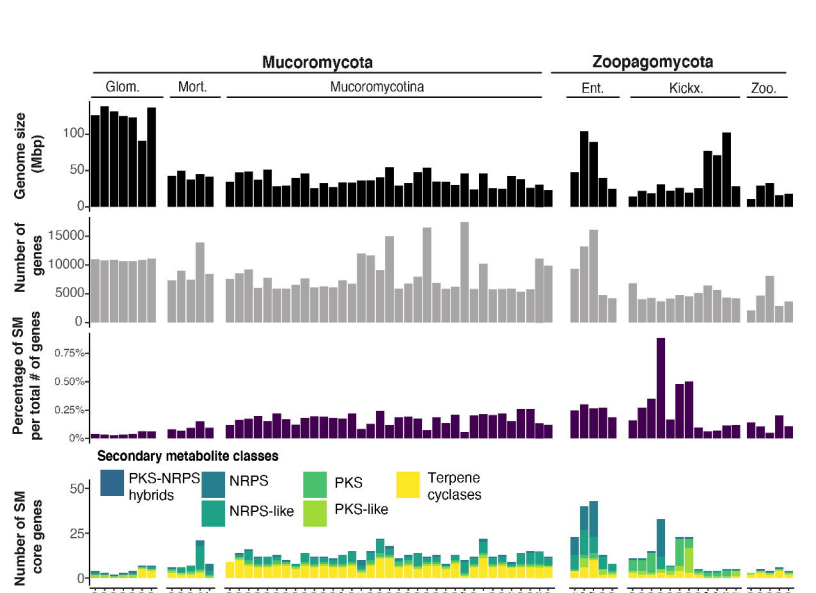


Figure 1. Genome size, number of genes, proportion of secondary metabolism (SM) gene clusters and number of predicted SM gene clusters for 66 Zoopagomycota and Mucoromycota sequenced genomes. Color code represents the category of SM predicted per isolate. NRPS: Non-ribosomal peptide synthetases. PKS: Polyketide synthases. Glom.: Glomeromycotina. Mort.: Morteriellomycotina. Ent.: Entomophtoromycotina. Kickx.: Kickxellomycotina. Zoo.: Zoopagomycotina

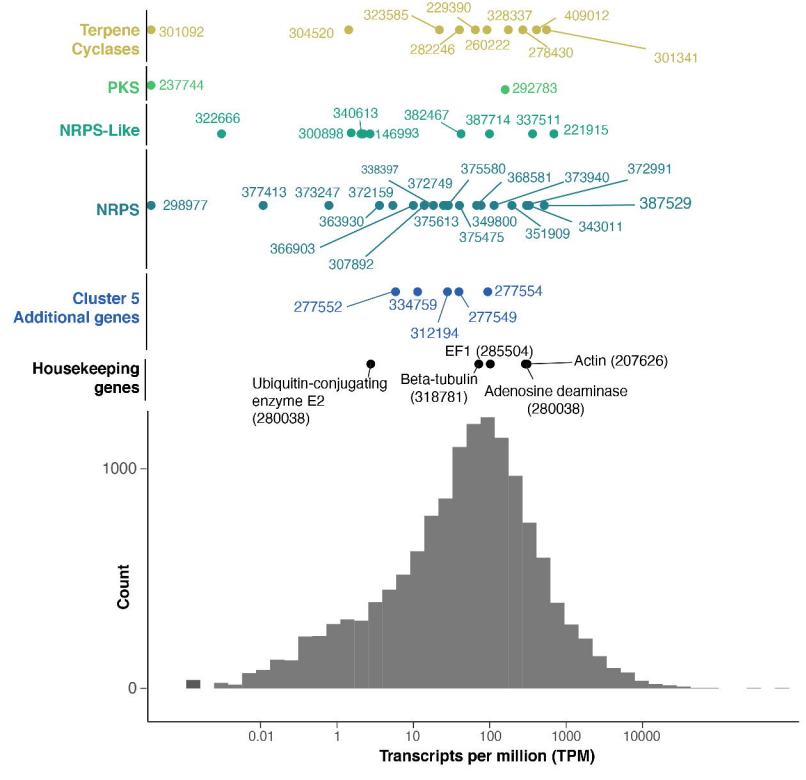


Figure 2. Distribution of number of RNAseq counts in transcripts per million (TPM) per genic feature from *B. meristosporus* CBS 931.73. Colors represent SM and genes of interest. X-axis represents the TPM count. Y-axis represents distribution of TPM. The scale is in log(TPM), and the values are in TPM absolute values. Histogram represents the distribution of mapped reads in TPM for all predicted gene models with non-zero TPM values across the *B. meristosporus* CBS 931.73 genome.

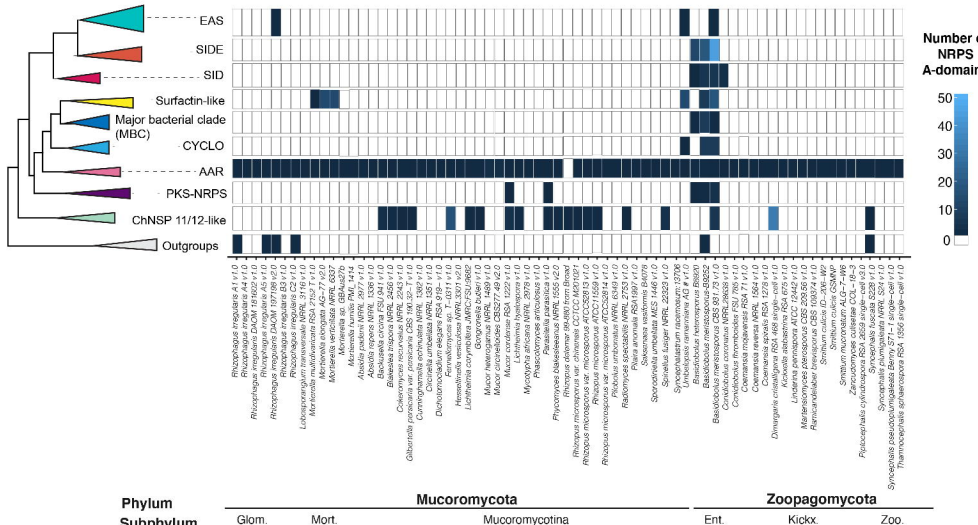


Figure 3. Phylogenetic sources and abundance of A-domains from NRPS predicted gene models for Zoopagomycota and Mucoromycota species. The maximum likelihood phylogenetic tree (left) represent a simplification of the reconstructed tree which includes the clades that include more than one A-domain from Mucoromycota/Zoopagomycota genomes. The heatmap (right) represents the abundances A-domains predicted for each domain clustered within each clade. *Basidiobolus* species are enriched in NRPS from the major bacterial clade (MBC), cyclosporin (CYCLO), surfactin-like, and siderophore (SIDE, SID) clades.

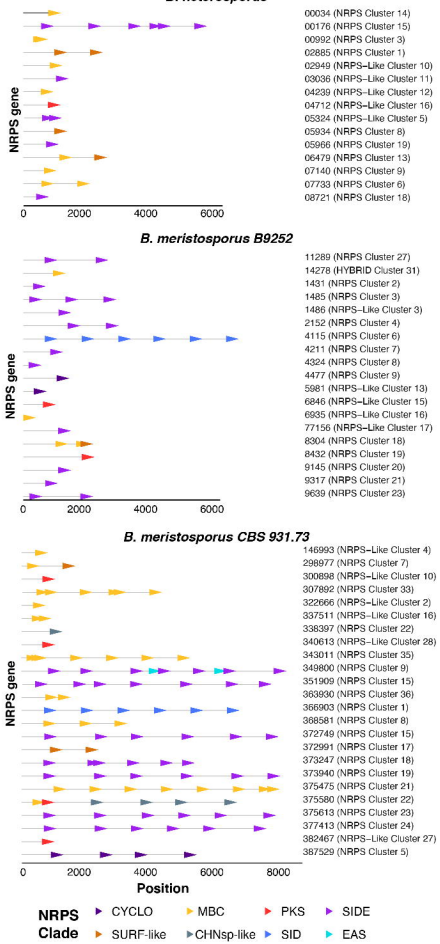


Figure 4. Graphical representation of the A-domains of each NRPS core gene predicted for *Basidiobolus* genomes. Horizontal grey lines represent the length of the predicted NRPS core gene. Arrows represent A-domains and are located in the position within the gene model. Colors represent the phylogenetic origin. Numbers represent the name of each gene model and predicted SM cluster for each genome.

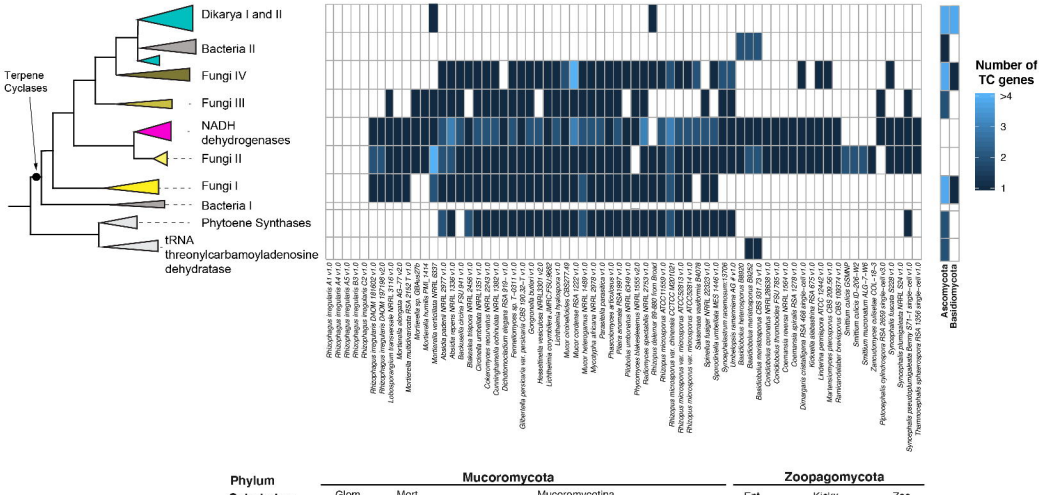


Figure 5. Phylogenetic sources and abundance of terpene cyclase (TC) core genes predicted for Zoopagomycota and Mucoromycota species. The maximum likelihood phylogenetic tree is a simplification of the maximum likelihood tree reconstructed using the TC core genes. The heatmap (right) represents the abundances of predicted TC genes within each reconstructed clade. Glom.: Glomeromycotina. Mort.: Morteriellomycotina. Ent.: Entomophtoromycotina. Kickx.: Kickxellomycotina. Zoo.: Zoopagomycotina

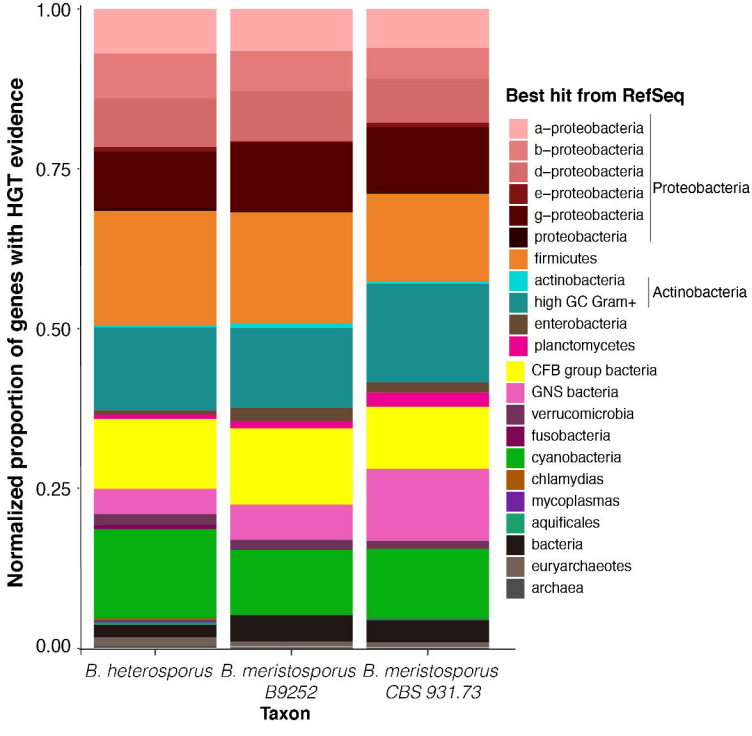


Figure 6. Plausible taxonomic sources of HGT genes. Bar-plot represents the proportion of diversity of HGT candidates for each *Basidiobolus* genome. Colors represent the taxonomy term for the RefSeq best hit from BLAST. Overall, between 3% to 5% of the gene models predicted for Basidiobolus species appear to be product of HGT from taxonomic groups of bacteria associated to reptilian and amphibian gut tracts (Proteobacteria, firmicutes, and CFB/bacterioidetes).

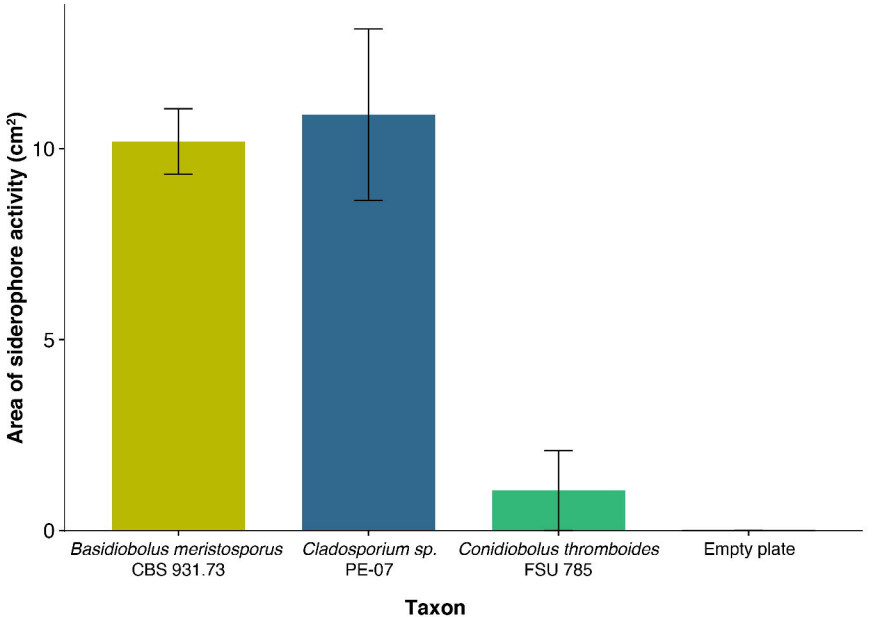


Figure 7. Siderophore activity of *Basidiobolus meristosporus* CBS 931.73 in a universal CAS assay using layered AY-CAS plates after 12 days. Bars represent mean siderophore activity measured per strain as the yellow area in AY-CAS plates for three replicates. Error bars represent the standard deviation for each replicate. *Cladosporium sp.* PE-07 represents the positive control. *Conidiobolus thromboides* FSU 785 represents a zygomycete with no evidence for siderophore NRPS expansion.